ACOUSTICAL ANALYSIS OF EXHAUST MUFFLERS FOR EARTH-MOVING MACHINERY

A THESIS SUBMITTED TO
THE GRADUATE SCHOOL OF NATURAL AND APPLIED SCIENCES
OF
MIDDLE EAST TECHNICAL UNIVERSITY

BY

TARIK OLĞAR

IN PARTIAL FULFILLMENT OF THE REQUIREMENTS
FOR
THE DEGREE OF MASTER OF SCIENCE
IN
MECHANICAL ENGINEERING

SEPTEMBER 2009

Approval of the thesis:

ACOUSTICAL ANALYSIS OF EXHAUST MUFFLERS FOR EARTH-MOVING MACHINERY

submitted by **Tarık OLĞAR** in partial fulfillment of the requirements for the degree of **Master of Science in Mechanical Engineering Department, Middle East Technical University** by,

Prof. Dr. Canan Özgen _____
Dean, Graduate School of **Natural and Applied Sciences**

Prof. Dr. Suha Oral _____
Head of Department, **Mechanical Engineering**

Prof. Dr. Mehmet Çalışkan _____
Supervisor, **Mechanical Engineering Dept., METU**

Prof. Dr. Eres Söylemez _____
Co-Supervisor, **Mechanical Engineering Dept., METU**

Examining Committee Members:

Prof. Dr. Eres Söylemez _____
Mechanical Engineering Dept., METU

Prof. Dr. Mehmet Çalışkan _____
Mechanical Engineering Dept., METU

Prof. Dr. Yusuf Özyörük _____
Aerospace Engineering Dept., METU

Prof. Dr. Reşit Soylu _____
Mechanical Engineering Dept., METU

Asst. Prof. Gökhan O. Özgen _____
Mechanical Engineering Dept., METU

Date: _____

I hereby declare that all information in this document has been obtained and presented in accordance with academic rules and ethical conduct. I also declare that, as required by these rules and conduct, I have fully cited and referenced all material and results that are not original to this work.

Name, Last name : Tarık Olğar

Signature :

ABSTRACT

ACOUSTICAL ANALYSIS OF EXHAUST MUFFLERS
FOR EARTH-MOVING MACHINERY

Olğar, Tarık
M.S., Department of Mechanical Engineering
Supervisor : Prof. Dr. Mehmet Çalışkan
Co-Supervisor: Prof. Dr. Eres Söylemez

September, 87 pages

This study concerns with acoustical analysis of exhaust mufflers for earth-moving machinery. The study arises from the fact that there is a need for further noise reduction emitted by earth-moving machinery produced by Hidromek Inc. in order to be on the safe side of the limits stated in European Noise Directive 2000/14/EC. The acoustical performance of the muffler is investigated both experimental and numerical means. A three-dimensional finite element method is performed to calculate the transmission loss. An experimental setup is also developed to measure the transmission loss. Chung-Blaser, two-source and two-load methods are applied to measure the transmission loss of single expansion chamber with extended inlet/outlet. The experimental setup is verified by comparing the test results obtained by two-load method with one-dimensional analytical solution obtained by transfer matrix method. Transmission loss of the muffler of interest, calculated by finite

element method is compared with the experimental results. Sound power level of earth-moving machinery and insertion loss of the muffler is measured to investigate the acoustical performance of the muffler. These results can then be served as guidance for the acoustical design of a muffler.

Keywords: Exhaust muffler, transmission loss, insertion loss, finite element method, excavator

ÖZ

İŞ MAKİNELERİ İÇİN EGZOZ SUSTURUCULARININ
AKUSTİK ANALİZİ

Olğar, Tarık
Yüksek lisans, Makina Mühendisliği Bölümü
Tez Yöneticisi : Prof. Dr. Mehmet Çalışkan
Ortak Tez Yöneticisi: Prof. Dr. Eres Söylemez

Eylül 2009, 87 sayfa

Bu çalışma, iş makineleri için egzoz susturucularının akustik analiziyle ilgilidir. Bu çalışma, 2000/14/EC Avrupa Birliği Gürültü Direktifinde belirtilen sınır değerlerde güvenli tarafta olmak için, Hidromek A.Ş. tarafından üretilen iş makinelerin çevreye yaydığı gürültünün ilave düşürülmesi ihtiyacından doğmuştur. Egzoz susturucusunun akustik performansı, numeriksel ve deneysel olarak incelenmiştir. Üç boyutlu sonlu elemanlar yöntemi, iletim kaybı hesaplanmasında uygulanmıştır. İletim kaybının ölçülmesi için ise bir deney düzeneği geliştirilmiştir. Chung-Blaser, iki-kaynak ve iki-yük yöntemleri uzatılmış giriş ve çıkış borulu tek genleşme odalı bir susturucunun iletim kaybı ölçümü için uygulanmıştır. Deney düzeneği, transfer matris yöntemiyle elde edilen tek boyutlu analitik çözümle iki-yük yönteminin test sonuçlarıyla karşılaştırılarak doğrulamıştır. Çalışmaya konu olan susturucunun sonlu elemanlar yöntemiyle hesaplanan iletim kaybı deneysel sonuçlarla karşılaştırılmıştır.

Egzoz susturucusunun akustik performansının incelenmesi için iş makinesinin ses gücü seviyesi ve susturucunun takma kaybı ölçülmüştür. Bu sonuçlar, susturucunun akustik tasarımı için yol gösterici olarak kullanılabilir.

Anahtar kelimeler: Egzoz susturucusu, iletim kaybı, takma kaybı, sonlu elemanlar yöntemi,ekskavatör

To My Family and Hüsniye

ACKNOWLEDGMENTS

I wish to express my deepest gratitude to Prof. Dr. Mehmet Çalışkan and Prof. Dr. Eres Söylemez for their guidance, advice, criticism, encouragements and insight throughout the research.

I would like to thank my friends Ferhan Fıçıcı, Cevdet Can Uzer, Erkal Özbayramoğlu, Boran Kılıç, Durmuş Ali Göztaş, Koray Serdar Tekin and Cemil Eşref Yürüklü for their help, suggestions and comments.

Finally, I would like to thank my family and Hüsniye for their support and encouragement.

This study was supported by Hidromek Inc.

TABLE OF CONTENTS

ABSTRACT iv
ÖZ vi
ACKNOWLEDGMENTS ix
LIST OF TABLES xii
LIST OF FIGURES xiii
LIST OF SYMBOLS AND ABBREVIATIONS xvi
CHAPTERS
1. INTRODUCTION 1
2. LITERATURE SURVEY 5
2.1 Analytical Methods 5
2.2 Numerical Methods 8
2.3 Experimental Methods 10
3. THEORY OF MUFFLERS 12
3.1 Transfer Matrix Method 12
3.2 Transfer Matrix Representation of a Uniform Tube 16
3.3 Muffler Performance Parameters 18
3.3.1 Insertion Loss 18
3.3.2 Transmission Loss 19
3.4 Transfer Matrix Representations of Transmission Loss 20
4. FINITE ELEMENT MODELING 22
4.1 Acoustical Modelling of Perforation 24
4.1.1 Verification for Acoustical Modelling of Perforation 27
4.2 Acoustical Modelling of Absorbent Materials 30
4.2.1 Verification of Modelling Absorbing Material 32
5. TRANSMISSION LOSS MEASUREMENT 37
5.1 Transmission Loss Measurement Techniques 37

5.1.1 Chung-Blaser Method [26] 37
5.1.2 Two-Source Method [28] 40
5.1.3 Two-Load Method [38] 44
5.2 Transmission Loss Measurement Setup 48
5.2.1 Test Equipments 48
5.2.2 Specifications of the Test Setup 49
5.2.3 Calibration of the Microphones 50
5.3 Validation of Transmission Loss Measurement Setup 52
6. CASE STUDY 59
6.1 Description of the Muffler 59
6.2 Numerical Analysis with Msc.Actran 60
6.3 Transmission Loss Experiment with Two-Load Method 62
6.4 Comparison between Experimental and Numerical Results 63
6.5 Effect of Temperature and Flow on Transmission Loss 64
7. EXPERIMENTAL RESULTS 66
7.1 Airborne Sound Power Level Determination 66
7.2 Insertion Loss Measurement 73
8. DISCUSSIONS AND CONCLUSIONS 79
8.1 Finite Element Modelling 79
8.2 Experimental Methods 80
8.3 Future Work 81
REFERENCES 83

LIST OF TABLES

TABLES

Table 2.1 – $\lambda_{m,n}$ values used for calculation of cut-on frequencies for a circular duct.....14
Table 7.1 – Sound power level of HMK 200W-3 with and without muffler (dBA).....69

LIST OF FIGURES

FIGURES

Figure 1.1 – General view of an excavator 2
Figure 1.2 – Basic noise sources of an excavator. 3
Figure 3.1 – Basic representation of transfer matrix method. 16
Figure 3.2 – Representation of a uniform tube 16
Figure 3.3 – Representation of insertion loss [29] 19
Figure 3.4 – Representation of transmission loss [29] 19
Figure 3.5 – Schematic showing for transmission loss for a muffler 20
Figure 4.1 – Schematically representation of a modal basis in Msc.Actran 23
Figure 4.2 – Schematic showing for transfer impedance of perforation 24
Figure 4.3 – Square grid perforation for Mechel's formula 26
Figure 4.4 – Schematic of the three-pass perforated muffler. 27
Figure 4.5 – Transmission loss of the three-pass perforated muffler [34] 28
Figure 4.6 – Transmission loss comparison for three-pass muffler 29
Figure 4.7 – Transmission loss results for three-pass perforated muffler with different mesh sizes 30
Figure 4.8 – A single-pass perforated absorbing muffler 32
Figure 4.9 – Transmission loss of single-pass perforated absorbing muffler [37] 33
Figure 4.10 – Comparison of the results obtained by two modelling approaches with experiment for single-pass perforated absorbing muffler 34
Figure 4.11 – Transmission loss results for the first modelling approach of single-pass perforated absorbing muffler 36
Figure 4.12 – Transmission loss results for the second modelling approach of single-pass perforated absorbing muffler 36
Figure 5.1 – Measurement setup of Chung-Blaser method 38

Figure 5.2 – Measurement setup of two-source method 40
Figure 5.3 –Transfer matrix relation between incident and reflected waves 44
Figure 5.4 – Measurement setup of two-load method..... 45
Figure 5.5 – Transmission loss measurement setup..... 48
Figure 5.6 – Configurations for microphone calibration 51
Figure 5.7 – Single expansion chamber with extended inlet/outlet 52
Figure 5.8 – Single expansion chamber with extended inlet/outlet 53
Figure 5.9 – Modulus of the calibration factor between the microphones..... 54
Figure 5.10 – Phase angle of the calibration factor between the microphones..... 54
Figure 5.11 – Comparison of experimental result obtained by Chung-Blaser method with 1-D solution and Msc.Actran prediction 55
Figure 5.12 – Comparison of experimental result obtained by two-source method with 1-D solution and Msc.Actran prediction 56
Figure 5.13 – Comparison of experimental result obtained by two-load method with 1-D solution and Msc.Actran prediction 57
Figure 5.14 – Comparisons of the experimental methods with 1-D Solution..... 57
Figure 6.1 – General view of the muffler on HMK 200W-3 wheeled excavator 60
Figure 6.2 – Muffler used on HMK 200W-3 wheeled excavator 61
Figure 6.3 – FE model of the muffler of interest 61
Figure 6.4 – Transmission loss setup used for the muffler of interest 62
Figure 6.5 – Transmission loss of the muffler of interest 63
Figure 6.6 – Temperature effect on transmission loss (FEA result) 65
Figure 6.7 – Flow effect on transmission loss (FEA result) 65
Figure 7.1 – Measurement points for sound power level test 67
Figure 7.2 – Installation configurations of the muffler for measurements 68
Figure 7.3 – A-weighted sound power level of the excavator with and without muffler up to 5 kHz 70
Figure 7.4 – A-weighted sound power level of the excavator with and without up to 1 kHz muffler 71
Figure 7.5 – Insertion loss of the muffler of interest in 1/3 octave bands..... 74

Figure 7.6 – Insertion loss measurement result for the muffler of interest up to 2.5 kHz 76
Figure 7.7 – Insertion loss measurement result for the muffler of interest up to1 kHz 77
Figure 7.8 – Comparison of measured insertion loss with transmission loss predicted by Msc.Actran 78

LIST OF SYMBOLS AND ABBREVIATIONS

SYMBOLS

a : Radius of a perforation hole

A : Complex amplitude of forward pressure wave

A_{ij} : (1 1)th entry of the transfer matrix of an acoustic element

A_p : Admittance of a perforation

B : Complex amplitude of reflected pressure wave; number of blade in a fan

$B_{i,j}$: (1 2)th entry of the transfer matrix of an acoustic element

c : Speed of sound

$C_{i,j}$: (2 1)th entry of the transfer matrix of an acoustic element

d_h : Diameter of a perforation hole

D : Diameter of a circular duct

$D_{i,j}$: (2 2)th entry of the transfer matrix of an acoustic element

f : Frequency

$f_{cylinder}$: Cylinder firing frequency

f_{fan} : Blade passage frequency of the fan

f_l : Lower frequency limit of the impedance tube

$f_{m,n}$: Cut-on frequency for a circular duct

f_{pump} : Operational frequency of the pump

f_u : Upper frequency limit of the impedance tube

f^c : Cut-off frequency

H_c : Calibration factor

H_{ij} : Transfer function

$\hat{H}_{i,j}$: Uncorrected transfer function

k : Wave number

$\tilde{k}$: Complex wave number

L : Length

L_p : Sound pressure level

L_w : Sound power level

m : Number of pumping events per rotation in pumps

N : Number of cylinders in an engine

M : Mach number

p : Complex acoustic pressure

P : Measured complex acoustic pressure

r : Sound pressure reflection factor at normal incidence

R : Resistivity of an absorbing material

R_p : Resistance of the impedance of a perforation

u : Acoustic particle velocity

s : Spacing between the microphones

S : Cross-sectional area of a duct, area of the hemispherical surface

S_{ii} : Auto spectrum

S_{ij} : Cross spectrum

T : Transfer matrix

t_w : Thickness of a perforated plate

v : Acoustic mass velocity

W_i : Incident sound power

W_t : Transmitted sound power

X_p : Reactance of the impedance of a perforation

Y : Characteristic impedance of a duct

Z : Transfer impedance of a perforation

$\tilde{Z}$: Complex characteristic impedance of an absorbing material

α : $(1\ 1)^{th}$ entry of the transfer matrix defined in two-load method

β : $(1\ 2)^{th}$ entry of the transfer matrix defined in two-load method

δ : $(2\ 1)^{th}$ entry of the transfer matrix defined in two-load method

Δ : Determinant of a matrix

Δt_w : Correction factor for thickness of a perforated plate

ϕ : Porosity of a perforation

γ : $(2\ 2)^{th}$ entry of the transfer matrix defined in two-load method

η : Dynamic viscosity of the medium

λ : Constant for determination of higher order mode

ρ : Density of the medium

ω : Angular velocity

Ω : Rotational speed

ζ : Non-dimensional acoustic impedance of a perforation

ABBREVIATIONS

BEM : Boundary Element Method

FEA : Finite Element Analysis

FEM : Finite Element Method

IL : Insertion Loss

TL : Transmission Loss

TMM : Transfer Matrix Method

CHAPTER 1

INTRODUCTION

Earth-moving machines are heavy-duty engineering vehicles designed for realization of engineering projects such as roads, dams, open pit excavation, quarries, and trenching, recycling, landscaping and building sites [1]. The most common types of earth-moving machines are: excavators, backhoe loaders, bulldozers, loaders, cranes, drilling machines and graders.

Excavator is a mobile machine, which is moved by the help of either crawler track or rubber-tired undercarriage, with an upper structure capable of continuous rotation [2]. Upper structure including boom, arm, bucket and cab is mounted on a rotating platform over an undercarriage with tracks or wheels (Figure 1.1). It is primarily designed for excavating with a bucket, without movement of the undercarriage during the work cycle. An excavator work cycle normally includes digging, elevating, swinging and discharging of the material [3]. According to their sizes and power ratings, they are used in various engineering applications with several types of attachments, like bucket, shovel, breaker, auger or grapple.

The noise emission to the environment by earth-moving machinery is important from occupational and environmental standpoints. Therefore, legislations are developed to protect the health and well being of citizens as well as to protect the environment. Legislation concerning environmental noise of excavators is published by European Council, called European Council Directive 2000/14/EC [4].

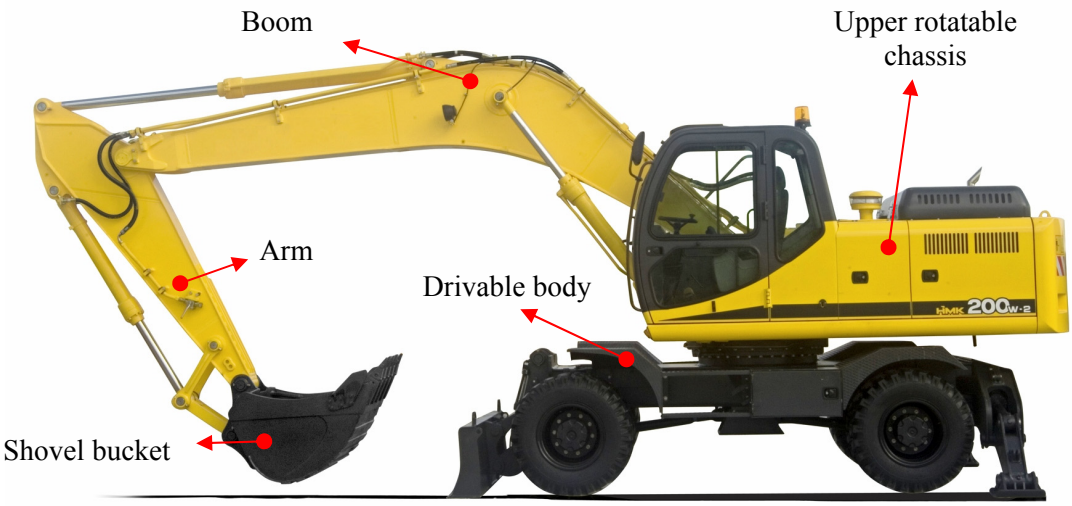

Figure 1.1 – General view of an excavator

The noise emission limits of excavators are declared in terms of permissible sound power level within this directive. These limits, which deviate from machine to machine by net engine power, are occasionally reduced 3 dBA. They are expected to be lowered even more in coming years.

Noise emitted by excavators is due to the combined contributions of various noise sources. The primary noise sources on excavators are typically the internal combustion engine body and transmission elements as mechanical noise sources; the exhaust, and engine cooling fan as aerodynamic noise source; and hydraulics pumps and lines as fluid-borne noise sources. These noise sources are shown schematically in Figure 1.2.

Among these noise sources, the exhaust noise is an important noise source. In order to comply with the laws of environmental protection and occupational safety, the exhaust noise should be controlled. Therefore, proper acoustical design of muffler becomes a priority in noise reduction efforts.

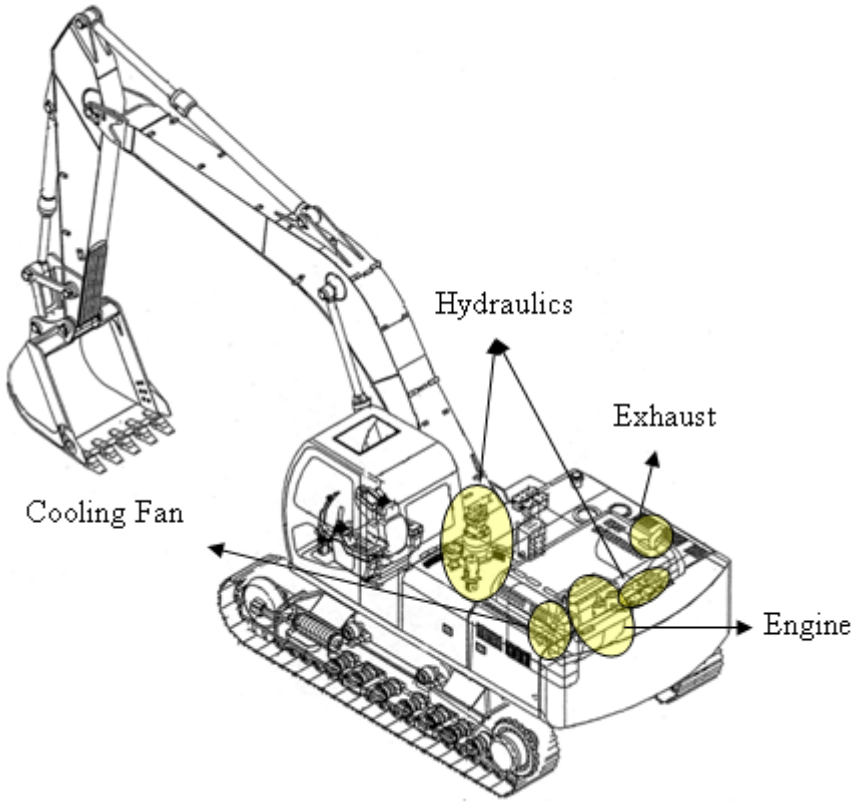

Figure 1.2 – Basic noise sources of an excavator

This study arises from the fact that there is a need for further noise reduction emitted by excavators produced by Hidromek Inc. in order to be on the safe side of the limits stated in European Noise Directive 2000/14/EC. Therefore, the objective of this study is acoustical evaluations of exhaust muffler leading to new design tips.

The material in the thesis is organized in eight chapters: Literature review of analytical, numerical and experimental methods used in acoustics of exhaust muffler is summarized in Chapter 2. Basic acoustical theory of mufflers which is mainly about transfer matrix method is presented in Chapter 3. Finite element modelling of mufflers is explained in Chapter 4. Acoustical modelling of perforations and sound absorbing material for the transmission loss prediction and verification of these modelling methods are presented in this chapter. Chapter 5 is about transmission loss

measurement. Three experimental methods are presented for transmission loss measurements, namely, Chung-Blaser method, two-source method and two-load method. The developed experimental setup and its validation are also presented in this chapter. Next chapter, Chapter 6, covers the numerical and experimental results for the transmission loss of the muffler under study. The effect of temperature and flow on transmission loss is also presented. Results of the sound power determination test and insertion loss measurements are given in Chapter 7. Finally, Chapter 8 consists of summary and conclusions of this study. Recommendations for further improvement in acoustical design of muffler are also projected in the last chapter.

CHAPTER 2

LITERATURE SURVEY

Acoustical design of mufflers has been a topic of great interest for many years, and a great deal of research has been conducted. This chapter is devoted to the literature review of studies on exhaust mufflers in the relevant areas of this study. The literature review is presented in three main sections. Firstly, analytical methods to predict the acoustical behaviour of mufflers are reviewed. Secondly, numerical methods used for acoustical modelling of the mufflers are presented. Finally, a review of literature on experimental methods for transmission loss is provided.

2.1 Analytical Methods

Different analytical methods to predict the acoustical performance of mufflers have been proposed for many years. The NACA report by Davis et al. [5] is one of the first comprehensive studies about exhaust mufflers. The study was about theoretical and experimental investigation of the attenuation characteristics of various types of mufflers, such as simple and multiple expansion chambers and resonator muffler. They used transmission line theory by assuming both continuity of pressure and continuity of volume velocity at the discontinuities to calculate the attenuation by these mufflers.

Igarashi et al. [6, 7] used a method of electrical equivalent network instead of equations of motion and continuity to the muffler elements. The transmission characteristics of mufflers were calculated with the application of two-port theory using four-pole parameters. After four-pole transmission matrices of some muffler

elements were presented, the transmission characteristics of these mufflers were proposed to be determined using the product of these matrices for each muffler element.

Sreenath and Munjal [8] presented an analogical electrical circuit for an exhaust muffler and used this analogy for the insertion loss prediction of mufflers for the first time. The state variables of acoustic pressure and mass velocity were described as analogous to voltage and current. The radiation impedance at the downstream end of the muffler and source characteristics of the engine was given analogous to the load impedance. Transfer matrix method was developed for evaluation of the insertion loss of the cascade acoustical elements in this study.

Most of the advances in the theory of exhaust mufflers have come after the implementation of transfer matrix method [9]. This method is based on the linear one-dimensional wave propagation in ducts and formulation of muffler elements in transfer matrices in analogy to electric filter theory. Flow effects have been neglected until Munjal [10] defined convective pressure and convective mass velocity to take into account of convective effect of incompressible mean flow. In this study, it was shown that these new set of state variables are linearly related to the classical acoustic pressure and acoustic mass velocity. In the literature, a large number of transfer matrices have been theoretically developed and reported. These transfer matrices including the flow effects have been compiled in a book by Munjal [11] and, more recently, in another book by Mechel [12].

One of the challenges of modelling mufflers by transfer matrix method is to model perforation elements. These are generally used to confine the mean flow in order to reduce the back-pressure to the engine and the flow generated noise inside the muffler. Sullivan and Crocker [13] presented the first study about perforation. Distributed parameter wall impedance approach was developed to predict the transmission loss of a concentric resonator without mean flow. The perforated element was modelled as a continuous element in this approach. The local pressure

difference over the perforation was related with the normal particle velocity via surface-averaged impedance. An empirical formulation for this perforation impedance was also proposed in this study. However, the formulation was only recommended for the perforated wall, of which porosity was not too different from the sample porosity used in the experiment.

Sullivan [14] also developed a segmentation approach for modelling perforation. In this study, muffler components were divided into several segments. Each segment was modelled as two straight hard pipes and a coupling branch to be described by a transfer matrix. Hence, four-pole parameters for through-flow, cross flow and reverse flow elements were derived.

One main difference between the distributed and segmentation approach is that continuity of acoustic momentum is usually imposed in distributed approach, whereas, continuity of acoustic energy is usually assumed in segmentation approach. Moreover, the distributed approach is mainly convenient for relatively simple perforated mufflers. However, the discrete approach through segmentation is more convenient to analyze advanced muffler systems because of numerical simplicity and flexibility [15].

Transfer matrix method is based on one-dimensional approach and higher order mode propagation is neglected; therefore, this may lead inaccuracies for the mufflers with large diameters or at high frequencies. Several studies have been developed on analytical approaches considering the higher order mode propagation in expansion chambers. Selamet and Radavich [16] investigated the effect of length on the acoustical attenuation performance of concentric expansion chambers by using a two-dimensional, axisymmetric analytical solution. It was shown that multidimensional effects begin to dominate at higher frequencies approaching that first radial mode.

Selamet and Ji [17] developed a three-dimensional analytical approach to investigate the effect of multidimensional wave propagation on the acoustic attenuation in circular asymmetric expansion chamber with offset inlet and outlet ducts. Since higher order modes excited at the inlet discontinuity do not have a sufficient length to decay in the expansion chamber, non-planar wave effects in the inlet and the outlet ducts on the transmission loss performance can be investigated with this study for a short expansion chamber. The study couples the continuity conditions of the acoustic pressure and particle velocity at the inlet and outlet with the orthogonality relations of Fourier–Bessel functions. Using the same analytical approach, the transmission loss of circular flow-reversing chambers was developed in another study by Selamet and Ji [18]. The effects of length-to-diameter ratio of the chamber and the relative locations of the inlet and outlet ducts on the acoustic attenuation performance of the flow-reversing chamber were investigated in this particular study.

2.2 Numerical Methods

Analytical methods used for prediction of the performance of mufflers are generally based on plane wave assumption. Thus, three-dimensional effects are neglected in the study of propagation of waves in mufflers. In the last decade, however, three-dimensional numerical analyses of mufflers have been employed for more accurate performance prediction and muffler designs. Finite Element Method (FEM) and Boundary Element Method (BEM) are especially useful for mufflers with complicated geometry and large cross-sectional area where the plane wave propagation is no longer valid for the frequency range of interest.

One of the first studies based on FEM for predicting the transmission loss in mufflers was the study by Young and Crocker [19]. They developed a numerical technique using the variation formulation of the acoustic field in mufflers. The transmission loss was predicted using four-pole network in which four-pole constants were calculated with FEM. The proposed technique was applied to a simple expansion

chamber for the plane wave region. The FEM result was shown to be in a reasonable agreement with plane wave solution. In another study by Young and Crocker [20], the same method was successfully applied to a flow-reversing muffler chamber. The validity of the proposed method was established experimentally by a number of different chambers. These two studies presented the possibility of accurate prediction of mufflers by FEM.

Bilawchuk and Fyfe [21] compared FEM and BEM methods for calculating the transmission loss in silencers. It was stated that FEM is more powerful than BEM, since computation is performed on the entire domain in FEM. In the study, transmission loss of an expansion chamber was calculated using three different methods; namely the traditional method, the four-pole transfer matrix method, and the three-point method with FEM and BEM. It was concluded that the combination of the finite element method and the three-point method is advantageous over other considered methods. It was also demonstrated that there is a good agreement between the FEM results with three-point method and the experimental results for an expansion chamber.

Wu et al.. [22] proposed an improved method for four-pole transfer matrix method using BEM. This method lowered the computation time in the prediction of transmission loss due to the necessity of only one BEM matrix calculation at each frequency for the boundary condition. The improved method has applied in the transmission loss prediction of two muffler models, a concentric tube resonator with a flow plug and two-duct perforated muffler using BEM with several different transfer impedance formulas. Transmission loss predictions were shown to be in reasonable agreement with the experimental results.

In another study by Wu et al.. [23], a three-dimensional direct mixed-body boundary element method was developed for packed silencers. This method is based on the multi-domain boundary element method which necessitates homogeneous and isotropic sub domains. The study also considered modelling of perforated plates and

two different acoustic media, i.e., air and absorbing material. The proposed formulation was verified by examination of several test cases and comparison of these cases with experimental results. Mehdizadeh and Paraschivoiu [24] implemented the finite element method to the test cases of the previous study by Wu et al.. [23]. Transmission loss of packed muffler and a parallel baffle silencer was predicted by modelling acoustic wave propagation in a non-homogeneous domain. Perforated plates were modelled as complex acoustic impedance and absorption lining were modelled with a complex speed of sound and density. It was shown that FEM results were in a good agreement with the experimental results for most of the frequencies.

2.3 Experimental Methods

The most important parameter that describes the acoustic performance of a muffler is transmission loss, since it is a property of muffler only. Although measurement of transmission loss is rather difficult than the calculation from the models, there has been great progress in experimental evaluation of the transmission loss in recent years.

Seybert and Ross [25] presented a two-microphone random excitation method to evaluate acoustical properties such as impedance and transmission loss. Two wall-mounted microphones were used in an upstream location between the source and the muffler .A third wall mounted microphone was used at the downstream. A white noise excitation was applied to the sound source. The incident and reflected acoustic waves were decomposed by measuring the auto spectral densities at three microphone location and also the cross spectral density between upstream microphones. The results for the transmission loss of a prototype automotive muffler were given for no flow cases. The advantage of the proposed method was that an acoustical property for the whole frequency range of interest with a specified resolution is found in a very short measurement time.

Chung and Blaser [26] presented a modification of the two microphone random excitation method. A transfer function approach was developed instead of considering the individual spectral densities. In this method, transfer function between the two upstream microphones was evaluated. The reflection coefficient was evaluated by using this transfer function and distance between the microphones. So, the transmission loss was determined using the complex reflection coefficients measured at two locations upstream and downstream of the muffler. It was also presented that experimental results were found to agree well with theoretical predictions.

Transmission loss of a muffler can be calculated using the four pole parameters which can be determined experimentally. Lung and Doige [27] used a transient testing technique to measure the four-pole parameters of uniform tubes, flare tubes, and expansion chambers. Two-load, four-microphone approach was proposed in the study. This method was based on transfer matrix approach. Two different loads were applied to the output of the system, and then, after application of the four-pole parameters matrix equation, four unknowns and four equations were obtained. However, this method becomes unstable if difference between the two loads approaches to zero.

Two-source method which is also based on transfer matrix was presented by Munjal and Doige [28]. This method is conceptually similar to the existing two-load method [27]. Two sound sources must be placed at two different configurations, firstly at the input of the system and then at the output. The form of equations relating the four parameters in terms of six measured transfer functions or pressure ratios is the same for both methods. The two-source method was shown to be functionally much more stable than two-load method and independent of the loads at the terminations.

CHAPTER 3

THEORY OF MUFFLERS

This chapter deals with mainly one dimensional theory of exhaust mufflers. The fundamentals of transfer matrix method that will be frequently used throughout the thesis are summarized in this chapter. The main assumptions and limitations of the transfer matrix method are also given. The insertion loss and transmission loss which are the parameters used for the acoustical performance of exhaust muffler are introduced and transfer matrix representation of the transmission loss is derived.

3.1 Transfer Matrix Method

An exhaust muffler consists of a duct system acting as a wave-guide in which the sound propagates. The sound propagation is assumed to be strictly fluid born; therefore, no structure-borne sound is concerned. This assumption holds, as the transmitted energy through the duct walls typically is small in comparison with the energy propagating in the duct. The sound pressure is typically less than one percent of the static pressure in exhaust mufflers and this correspond to sound pressure level around 130-150 dB, in air at normal atmospheric pressure level [29]. Therefore, the sound field in mufflers can be assumed as linear. These assumptions allow the sound field of the mufflers in an inviscid stationary medium to be governed by Helmholtz equation [11]

$$\nabla^2 p - k^2 p = 0 \tag{3.1}$$

where $k = \frac{\omega}{c}$ is wave number, ω is angular frequency, c is the speed of sound and p is the acoustic pressure in the frequency domain.

The main part of the acoustic energy in an exhaust system comes from the engine pulsations and has low frequency content. In particular, the wavelength for the pulsations is normally much longer than the diameter of the main exhaust pipe. This implies that the sound field in an exhaust muffler primarily consists of plane waves. A plane wave is defined in such way that the pressure across a duct cross section is constant. This is valid when the wavelength of the travelling wave is much longer than the largest cross-sectional dimension of the duct. When the wavelength decreases and becomes of the same order as the cross-sectional dimension, higher order modes may start to travel in the duct. The cut-on frequencies, $f_{m,n}$ for a circular duct can be found as [30],

$$f_{m,n} = \lambda_{m,n} \frac{c}{\pi D} \tag{3.2}$$

where $\lambda_{m,n}$ is can be found from Table 2.1. The subscripts "m" and "n" indicate circumferential mode number and radial mode number, respectively. The modes corresponding to m=0 are axisymmetric and the mode correspond to m=0 and n=0 is a plane wave.

Therefore, for a circular duct, only plane waves are present up to the cut-off frequency [11]

$$f^c = 1.84 \frac{c}{\pi D} \tag{3.3}$$

where D is the diameter of the duct cross-section.

Table 2.1 – $\lambda_{m,n}$ values used for calculation of cut-on frequencies for a circular duct

n \ m	**0**	**1**	**2**	**3**
0	0	1.84	3.05	4.2
1	3.83	5.33	6.71	8.02
2	7.02	8.54	9.97	11.35
3	10.17	11.71	13.17	14.59

Since the wave propagation is assumed as one dimensional (plane wave propagation), the sound field in a muffler can be described as the linear, one-dimensional wave equation, e.g. the z-direction in a duct.

$$\frac{\partial^2 p}{\partial z^2} - k^2 p = 0 \tag{3.4}$$

The solution of the Equation (3.4) can be given as:

$$p = Ae^{-jkz} + Be^{+jkz} \tag{3.5}$$

In Equation (3.5), p is the sum of two plane waves, one travelling in the positive z direction with amplitude A and the other in the negative z direction with B.

For a plane wave moving along a duct, one could define mass velocity

$$v = \rho S u \tag{3.6}$$

where ρ is the density of the medium, S is the cross sectional area of the duct and u is the acoustic particle velocity.

Hence, acoustic mass velocity can be determined as:

$$v = \frac{1}{Y}(Ae^{-jkz} - Be^{+jkz}) \tag{3.7}$$

where Y is the characteristic impedance of the duct, defined by $Y = \frac{c}{S}$, which is the ratio of the acoustic pressure and mass velocity of a plane progressive wave.

The muffler can be described by acoustic two-port method in the form of transfer matrix when the sound field in a muffler is linear and the plane wave is propagated at the inlet and outlet sections of the muffler. Therefore, muffler can be treated as a time-invariant, linear and passive two-port with appropriate input and output state variables. Transfer matrix formulation is developed by choosing acoustic pressure and acoustic velocity (particle, volume or mass velocity) at the inlet and outlet sections of the muffler, respectively, as input and output state variables. This method, called Transfer Matrix Method, especially suited to treat problems with one preferred direction for the acoustic energy flow as in exhaust systems [31]. Therefore, the transfer matrix representation (four-pole parameter representation) of a muffler can be written as:

$$\begin{bmatrix} p_u \\ v_u \end{bmatrix} = \begin{bmatrix} T_{11} & T_{12} \\ T_{21} & T_{22} \end{bmatrix} \begin{bmatrix} p_d \\ v_d \end{bmatrix} \tag{3.8}$$

where subscripts “u” and “d” indicate upstream and downstream variables, respectively. The sound pressure p_u and mass velocity v_u on the inlet side of the muffler can be fully transferred to the sound pressure outlet p_d and v_d on the outlet side of the muffler by using transfer matrix T, which consists of the four elements T_{11}, T_{12}, T_{21} and T_{22}. This is shown schematically in Figure 3.1.

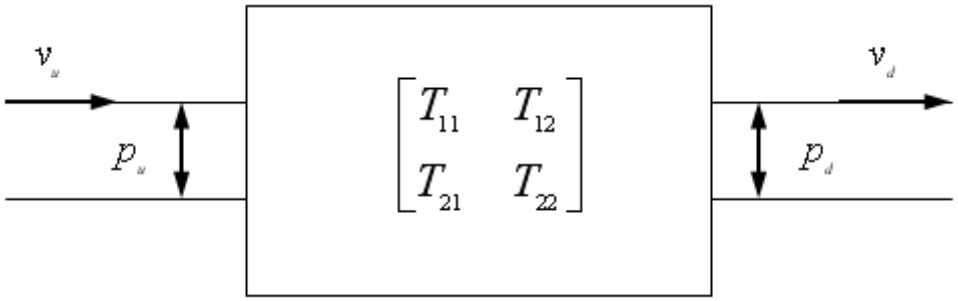

Figure 3.1 – Basic representation of transfer matrix method.

3.2 Transfer Matrix Representation of a Uniform Tube

One of the basic elements used extensively in mufflers is a uniform tube. Transfer matrix representation of this element is derived as an example. Other muffler elements, such as sudden expansions, sudden contractions, extended tubes, concentric resonators can be derived from basic equations similarly.

For plane wave propagation in a uniform tube of length L, constant cross section S, the sound pressure p and the acoustic mass velocity v anywhere in the pipe element can be represented as the sum of left and right travelling waves.

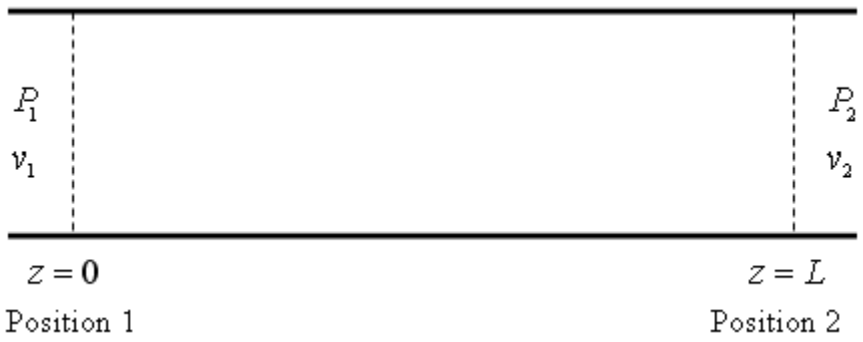

Figure 3.2 – Representation of a uniform tube

From Equation (3.5) and Equation (3.7), the sound pressure p_1 and acoustic mass velocity v_1 at position 1 (upstream end) is

$$p_1 = A + B \tag{3.9}$$

$$v_1 = \frac{1}{Y}(A - B) \tag{3.10}$$

The sound pressure p_2 and acoustic mass velocity v_2 at position 2 (downstream end) can be found in same manner as:

$$p_2 = Ae^{-ikL} + Be^{ikL} \tag{3.11}$$

$$v_2 = \frac{1}{Y}(Ae^{-ikL} - Be^{ikL}) \tag{3.12}$$

By using Equation (3.9) and Equation (3.10), p_2 and v_2 can be obtained in terms of p_1 and p_2 as:

$$\begin{aligned} p_2 &= (A + B)\cos(kL) - i(A - B)\sin(kL) \\ &= p_1 \cos(kL) - iYv_1 \sin(kL) \end{aligned} \tag{3.13}$$

$$\begin{aligned} v_2 &= \frac{A - B}{Y}\cos(kL) - i(\frac{A + B}{Y})\sin(kL) \\ &= v_1 \cos(kL) - i\frac{p_1}{Y}\sin(kL) \end{aligned} \tag{3.14}$$

Equation (3.13) and Equation (3.14) can be written as in the matrix form:

$$\begin{bmatrix} p_2 \\ v_2 \end{bmatrix} = \begin{bmatrix} \cos(kL) & -iY\sin(kL) \\ -i\sin(kL)/Y & \cos(kL) \end{bmatrix} \begin{bmatrix} p_1 \\ v_1 \end{bmatrix} \tag{3.15}$$

This can be inverted to obtain the desired transfer matrix relation of a uniform tube as:

$$\begin{bmatrix} p_1 \\ v_1 \end{bmatrix} = \begin{bmatrix} \cos(kL) & iY\sin(kL) \\ i\sin(kL)/Y & \cos(kL) \end{bmatrix} \begin{bmatrix} p_2 \\ v_2 \end{bmatrix} \tag{3.16}$$

3.3 Muffler Performance Parameters

There are several parameters that describe the acoustic performance of a muffler. The most important ones are the insertion loss (IL) and the transmission loss (TL), which are explained below.

3.3.1 Insertion Loss

Insertion loss is the difference between the sound pressure levels measured at the same reference point from the termination without and with the muffler as shown in Figure 3.3. Insertion loss can be expressed as:

$$IL = L_{p2} - L_{p1} \tag{3.17}$$

Insertion loss can be measured by using a single microphone mounted outside of the exhaust system in free space without and with muffler in place. It does, however, depend on both upstream acoustic source characteristics and downstream acoustic load characteristics.

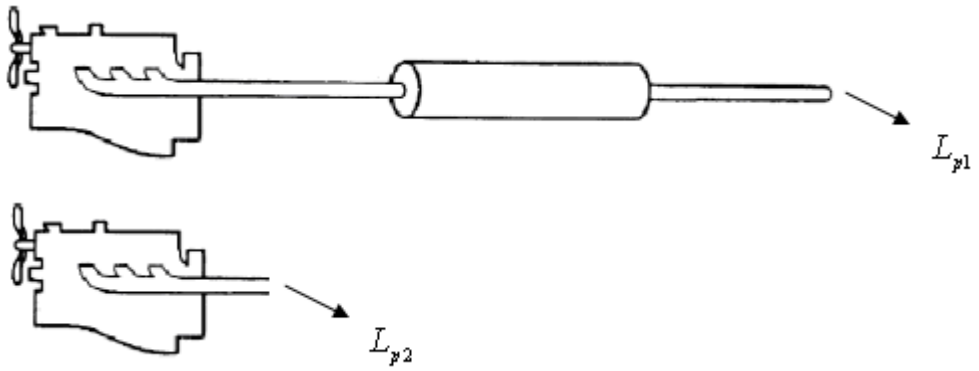

Figure 3.3 – Representation of insertion loss [29]

3.3.2 Transmission Loss

The transmission loss is defined as the ratio between the sound power incident to the muffler (W_i) and the transmitted sound power (W_t) for the case that there is a reflection-free termination on the downstream side as shown in Figure 3.4. Transmission loss can be expressed as:

$$TL = 10\log(W_i / W_t) \tag{3.18}$$

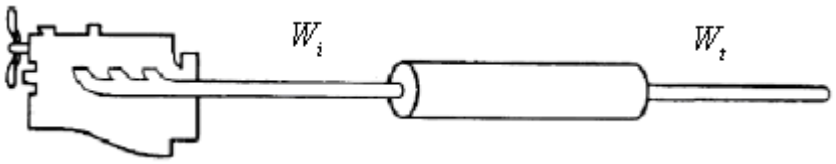

Figure 3.4 – Representation of transmission loss [29]

Transmission loss is a property of the muffler only and does not depend upon upstream acoustic source and downstream acoustic load characteristics. Transmission

loss is more difficult to measure than insertion loss due to the anechoic termination and the determination of sound power incident directly on the muffler.

3.4 Transfer Matrix Representations of Transmission Loss

The sound pressure wave at the upstream and downstream side of the muffler can be decomposed into the progressive wave components as shown in Figure 3.5. A_u, and B_u are acoustic pressures associated with incident and reflected wave at the upstream side, respectively. A_d is the acoustic pressure associated with transmitted wave at the downstream side. There is no reflected wave at the downstream of the muffler due to the anechoic termination.

Figure 3.5 – Schematic showing for transmission loss for a muffler

Transmission loss can also be described in terms of the progressive wave components as:

$$\begin{aligned} TL &= 10\log\left|\frac{S_u A_u^{\,2}}{S_d A_d^{\,2}}\right| \\ &= 20\log\left|\frac{A_u}{A_d}\right| + 10\log\left|\frac{S_u}{S_d}\right| \end{aligned} \tag{3.19}$$

where S_d and S_u are the cross-section of the muffler at the downstream and upstream side, respectively.

Acoustic pressure and mass velocities in the upstream and downstream of the muffler can be described in terms of the incident, reflected and transmitted wave as below.

$$p_u = A_u + B_u \tag{3.20}$$

$$v_u = \frac{1}{Y_u}(A_u - B_u) \tag{3.21}$$

$$p_d = A_d + B_d = A_d \quad (B_d = 0) \tag{3.22}$$

$$v_d = \frac{1}{Y_d}(A_d - B_d) = \frac{A_d}{Y_d} \tag{3.23}$$

Thus,

$$\begin{aligned} A_u &= (p_u + Y_u v_u)/2 \\ &= [(T_{11}A_d + T_{12}\frac{A_d}{Y_d}) + Y_d(T_{21}A_1 + T_{22}\frac{A_1}{Y_1})]/2 \end{aligned} \tag{3.24}$$

Therefore, transmission loss is defined by

$$TL = 20\log\left|\frac{T_{11} + T_{12}/Y_d + Y_u T_{21} + (Y_d/Y_u)T_{22}}{2}\right| + 10\log\left|\frac{S_u}{S_d}\right| \tag{3.25}$$

CHAPTER 4

FINITE ELEMENT MODELING

FEM has become a practical technique for acoustical analysis and solution of noise problems. One area that has been successfully used in recent years is the design of mufflers for noise control. The conventional transfer matrix method for the acoustical analysis of mufflers is of limited use, since it cannot be applied to mufflers which have complicated internal structures. However, FEM can perform computations on the entire domain of the muffler, and therefore; it is a more powerful tool for performance prediction and muffler design.

Finite element modelling of mufflers in this study generally consists of the following steps. A solid model of the muffler is built using computer-aided design software. Pro/ENGINEER is used in this study for this purpose. The second step is to build the finite element model which is formed by dividing the interior domain of the muffler into a large number of elements. Element size is significant for the accuracy of analysis and should be selected depending on the highest frequency of interest. It is recommended that elements are generated in such a way that at least 6 linear elements are formed per wavelength corresponding to the highest frequency of interest [32]. Therefore, the acoustic cavity of the muffler is meshed accordingly in the pre- and post- processing software Msc.Patran. After the mesh is defined, the fluid properties for the acoustic domain should be specified. If necessary, boundary conditions which define generally how the acoustic fluid is excited should also be specified. Finally, the acoustical analysis is performed by Msc.Actran, which is a vibro-acoustic solver.

The modal basis, which is a feature provided by Msc.Actran is used in finite element modelling of a muffler. In modal basis, acoustic field of the muffler modelled by finite elements is coupled to an analytical representation of the acoustic field in a semi infinite duct at input and output of the muffler as shown in Figure 4.1. This coupling is made through the modal surface, defining the free faces of the elements to be coupled to this analytical representation. An excitation of unit intensity incident plane wave is applied to the semi-infinite duct at the inlet of the muffler. Msc.Actran then calculates the reflected and transmitted power of the waves even if they are not plane waves. Hence, transmission loss of the muffler can be calculated from the incident and transmitted power.

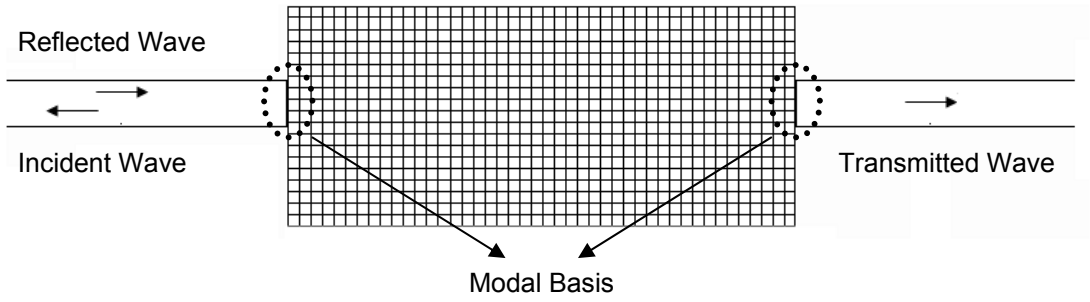

Figure 4.1 – Schematically representation of a modal basis in Msc.Actran

Acoustic analysis of muffler taking the flow into account can also be performed in Msc.Actran by applying the flow at the inlet modal surface of the muffler. The flow computed by Msc.Actran is assumed to be incompressible and irrotational.

Main sources of difficulties in finite element modelling of exhaust muffler are due to the perforated elements and absorption materials. The modelling techniques in the perforated elements and absorption material in Msc.Actran and their verification with literature are demonstrated in the following two parts.

4.1 Acoustical Modelling of Perforation

The perforated elements in the mufflers can be modelled by equivalent transfer impedance approach. The perforated element is replaced by an equivalent porous surface with known transfer impedance in this approach. This impedance is dependent on the perforation geometry (porosity, shape and size of holes, wall thickness, and hole pattern), the flow field (glazing and through flow), and the medium in contact with the perforation [33]. As shown in Figure 4.2, the main assumption of the equivalent transfer impedance approach is that the particle velocity is continuous on both sides of the perforated element while the sound pressure is not continuous.

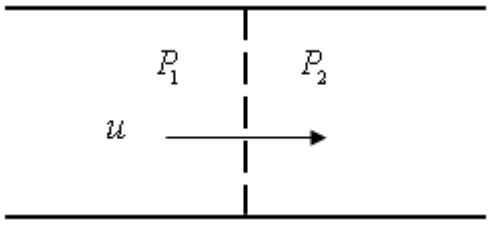

Figure 4.2 – Schematic showing for transfer impedance of perforation

The transfer impedance boundary condition is defined at the perforated element as:

$$Z = \frac{p_1 - p_2}{u} \tag{4.1}$$

where Z is the transfer impedance of the perforation, p_1 and p_2 are the sound pressures on each side of the element, and u is the particle velocity. Therefore, non-dimensional acoustic impedance of a perforated plate is defined as:

$$\zeta = \frac{p_1 - p_2}{\rho c u} \tag{4.2}$$

The complexity of the perforation impedance confines the analytical approaches only to simple perforations. Thus, experimental methods are generally applied to obtain the impedance such as the empirical formula by Sullivan and Crocker [13], which has been widely used in literature. Sullivan's formula is

$$\zeta = \frac{1}{\phi}\left[0.006 + ik(t_w + 0.75d_h)\right] \tag{4.3}$$

where ϕ is the porosity of the perforation, t_w is the wall thickness and d_h is the hole diameter.

Transfer admittance boundary condition, which is based on Mechel's formula, is recommended to model a perforated plate in Msc.Actran [34]. The perforated element is replaced by an interface coupled with the transfer admittance matrix given by Equation (4.4)

$$\begin{bmatrix} u_1^n \\ u_2^n \end{bmatrix} = \begin{bmatrix} A_p & -A_p \\ -A_p & A_p \end{bmatrix} \begin{bmatrix} p_1 \\ p_2 \end{bmatrix} \tag{4.4}$$

u_1^n and p_1 are the normal velocity and pressure on the first surface of the perforated element, while u_2^n and p_2 are the normal velocity and pressure on the second surface of the perforated element. The admittance of the perforation is defined as:

$$A_p = \frac{1}{R_p + iX_p} \tag{4.5}$$

where R_p and X_p are the resistance and reactance of the impedance of the perforation. Resistance and reactance values are obtained using Mechel's formula as:

$$R_p = \frac{1}{\phi}\sqrt{16\pi f \eta \rho}\left(1 + \frac{t_w}{2a}\right) \tag{4.6}$$

$$X_p = \frac{2}{\phi}\pi f \rho (t_w + 2\Delta t_w) \tag{4.7}$$

where a is the radius of the perforation hole, Δt_w is the correction factor, η is the dynamic viscosity of the medium. Porosity and correction factor depend of the grid geometry. These factors are expressed in Equations (4.8) and Equation (4.9) for a square grid shown in Figure 4.3.

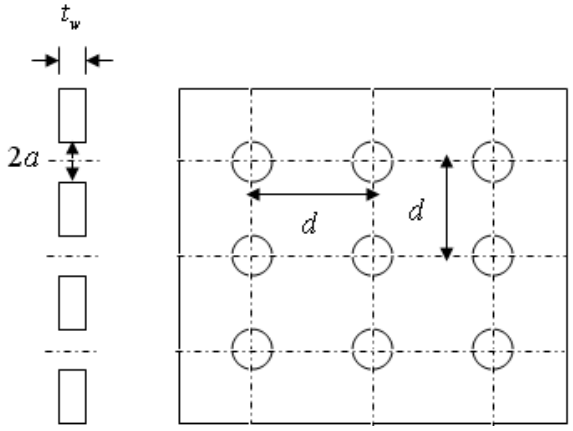

Figure 4.3 – Square grid perforation for Mechel's formula

$$\phi = \frac{\pi \cdot a^2}{d^2} \tag{4.8}$$

$$\Delta t_w = \begin{cases} 0.85 \cdot a\left(1 - 2.34\dfrac{a}{d}\right) & 0 < \dfrac{a}{d} < 0.25 \\ 0.668 \cdot a\left(1 - 1.9\dfrac{a}{d}\right) & 0 < \dfrac{a}{d} < 0.25 \end{cases} \tag{4.9}$$

where d is the distance between the centres of the perforation holes.

4.1.1 Verification for Acoustical Modelling of Perforation

Finite element modelling of perforated elements with Msc.Actran using Mechel's formula is verified through comparison with the results of the study performed by Ji and Selamet [35]. In this study, three-pass muffler with uniform perforation shown in Figure 4.4 is used.

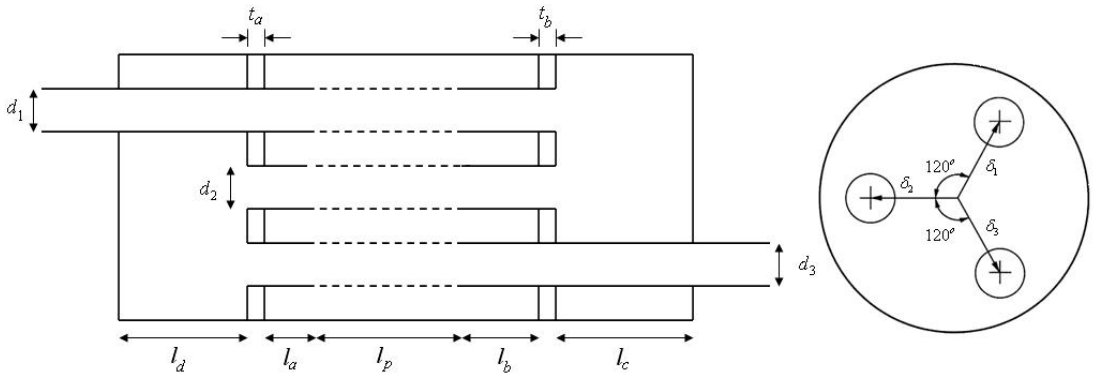

Figure 4.4 – Schematic of the three-pass perforated muffler.

The study considers $d_4 = 165.1$ mm for the chamber inner diameters, $d_1 = d_2 = d_3 = 48.9$ mm for the duct inner diameters, $\delta_1 = \delta_2 = \delta_3 = 39.7$ mm for the duct offset distances from the centre of chamber, $t = 0.8$ mm for the duct thickness, $t_a = t_b = 12.7$ mm for the baffle thickness. An interior duct porosity of $\phi = 0.045$

was obtained by 448 holes of $d_h = 2.34$ mm in each duct over the central region such that $l_p = 274$ mm and $l_a = l_b = 27.9$ mm.

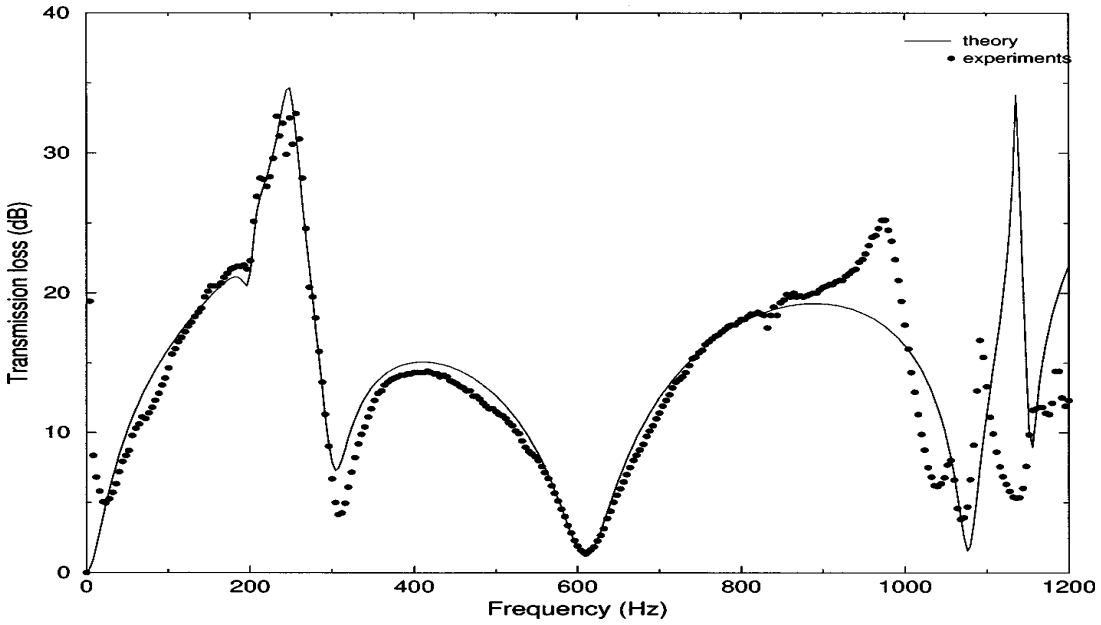

Figure 4.5 – Transmission loss of the three-pass perforated muffler [34]

In this study, three-pass perforated muffler is divided into a number of substructures and then BEM is applied to each one of the substructures leading a system of equations in terms of sound pressure and particle velocity. Using boundary condition and continuity equations, the transfer impedance matrix is obtained between the inlet and outlet of the muffler, yielding the four-pole parameters and the transmission loss. Sullivan's formula, which is given in Equation (4.3), is used for the acoustic impedance of perforation in theoretical calculation. Moreover, the transmission loss characteristics of the prototype three-pass perforated is measured in an impedance tube setup. Figure 4.5 shows the comparison between the theoretical prediction and the experimental results.

In this study, the transmission loss calculation of the same three-pass muffler is also performed with Msc.Actran. The FE model used in the analysis is composed of 29821 hexahedral elements and 24887 nodes as shown. The perforation is modelled by transfer admittance boundary condition. Mechel's formula is used for the calculation of the acoustic impedance of the perforation.

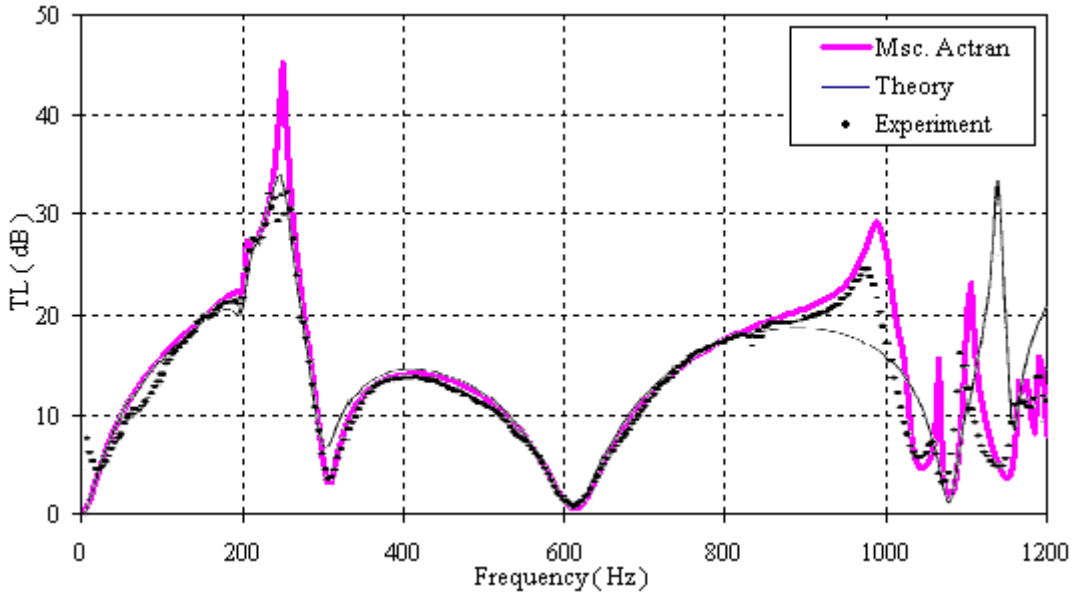

Figure 4.6 – Transmission loss comparison for three-pass muffler

FEM prediction by Msc.Actran for the transmission loss is compared with the result of the study by Ji and Selamet [34] in Figure 4.6. FEM result by Msc.Actran with Mechel's formula matches closely the experimental result through the frequency range of interest. There are only small differences in the peaks of the transmission loss curve. Therefore, transfer admittance boundary condition with Mechel's formula is to be used for modelling the perforation throughout the study.

In order to understand the sufficiency of total number of elements used, convergence test is to be carried out. Therefore, an additional analysis by using 82220 hexahedral elements and 71139 nodes has been performed. Transmission loss results from these

two analysis are compared in Figure 4.7. There is nearly no difference between the results obtained from the models with different mesh sizes at the frequency range of interest. Hence, it is confirmed that a fine enough element discretization has been used in the finite element model for the three-pass muffler.

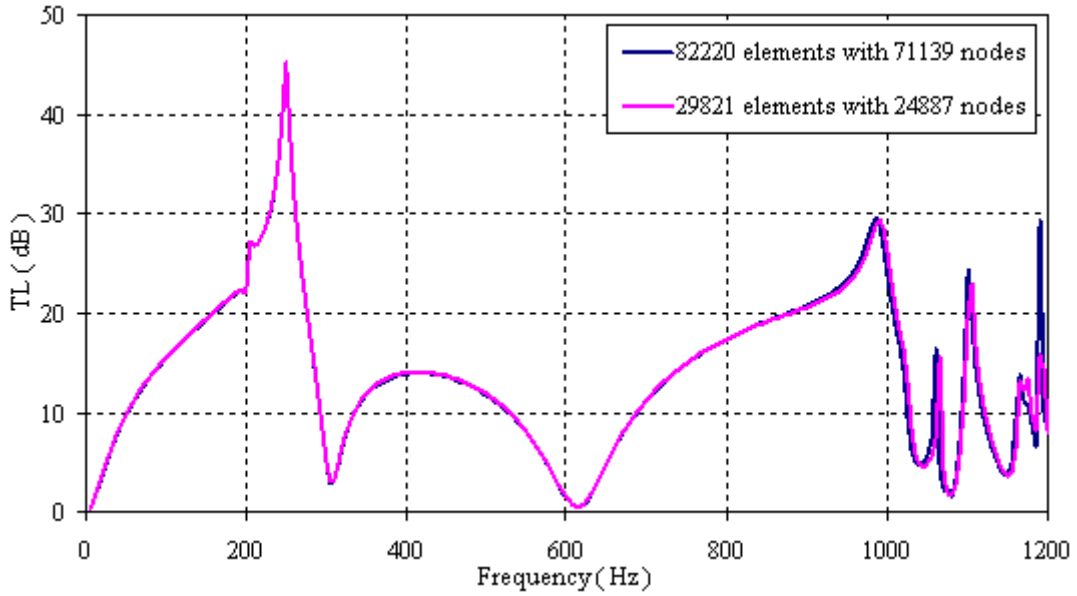

Figure 4.7 – Transmission loss results for three-pass perforated muffler with different mesh sizes

4.2 Acoustical Modelling of Absorbent Materials

Sound absorbing materials, such as glass fibers, foam, and mineral wool are generally used in mufflers. Their physical and acoustical properties are essential for the acoustical performance of mufflers. Sound is absorbed in fibrous material due to viscous friction and dissipation, which are expressed in terms of complex characteristic impedance and complex wave number. These properties should be determined by experiments due to the complex structure of fibrous material. However, empirical formulations are generally used due to the lack of information.

Delany and Bazley [36] presented empirical expressions which has been widely used in literature for complex characteristic impedance and complex wave number of an absorbing material

$$\frac{\tilde{Z}}{Z}=\left[1+0.051\left(\frac{f}{R}\right)^{-0.75}\right]+i\left[-0.0768\left(\frac{f}{R}\right)^{-0.73}\right] \tag{4.10}$$

$$\frac{\tilde{k}}{k}=\left[1+0.0858\left(\frac{f}{R}\right)^{-0.70}\right]+i\left[-0.1749\left(\frac{f}{R}\right)^{-0.59}\right] \tag{4.11}$$

where R is the resistivity, which is defined as the ratio of the pressure difference across a unit length of absorbing material to the flow velocity.

Sound absorbing materials are generally used in combination with perforated elements. Therefore, the acoustic impedance of perforation in contact with air-fibrous material should be considered in acoustic modelling of exhaust mufflers. This impedance is different from the acoustic impedance of perforations in contact with air only due to the influence of the sound absorbing material. Sullivan's formula and Mechel's formula have been developed for the perforation facing air-air contact without taking the effects of the fibrous material.

Sullivan's formula has been later modified for the perforations facing air-fibrous material by Selamet [37]:

$$\zeta=\frac{1}{\sigma}\left[0.006+ik(t_w+0.375d_h(1+\frac{\tilde{Z}}{Z}\frac{\tilde{k}}{k}))\right] \tag{4.12}$$

The effect of absorbent material is considered with the complex characteristic impedance $\tilde{Z}$ and complex wave number $\tilde{k}$ of the material.

4.2.1 Verification of Modelling Absorbing Material

In order to verify the modelling of sound absorbing material in Msc.Actran, a single-pass perforated muffler is analyzed and compared to the results in literature, obtained by Selamet et al. [37]. The schematic of the single-pass perforated muffler is shown in Figure 4.8.

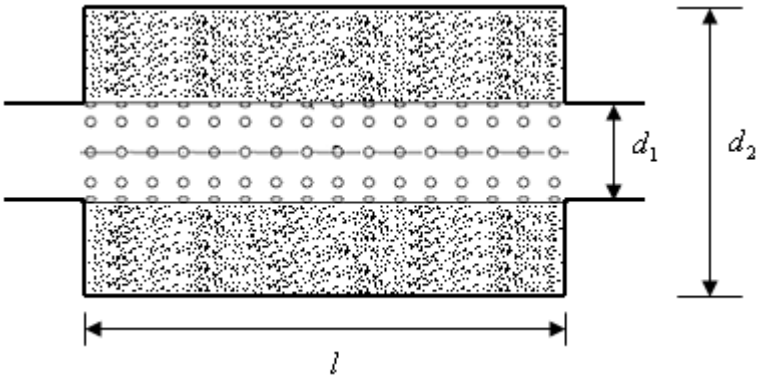

Figure 4.8 – A single-pass perforated absorbing muffler

The study considers a single-pass concentric muffler of length $l = 257.2$ mm with a uniformly perforated duct with porosity $\phi = 2\%$. The outer diameters are $d_1 = 49$ mm and $d_2 = 164.4$ mm. The diameter of the perforation hole is $d_h = 2.49$ mm. The thickness of perforated wall is $t_w = 0.9$ mm. The filling density of the sound absorbing material is 100 g/L and the flow resistivity is 4896 Rayls/m.

In this study, Equation (4.12) was used for the perforation impedance in contact with air-fibrous material. Acoustic properties of the sound absorbing material were determined experimentally and the measured complex impedance and wave number was used instead of the empirical expression by Delany and Bazley [36]. The study predicted the transmission loss of the single-pass perforated muffler by one-

dimensional analytical method and boundary element method. The results were compared with the experimental result and presented as shown in Figure 4.9.

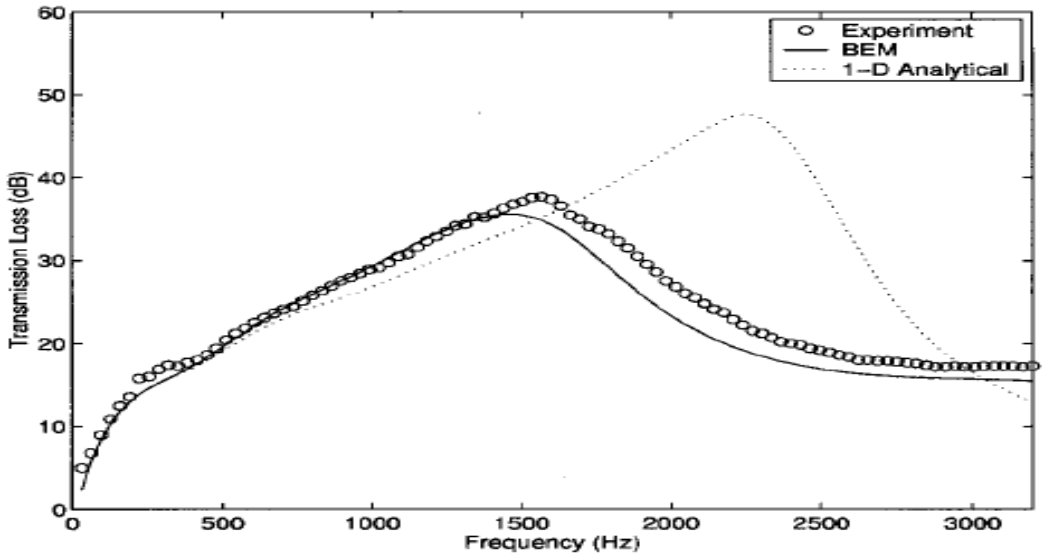

Figure 4.9 – Transmission loss of single-pass perforated absorbing muffler [37]

Two different modelling approaches are developed for the analysis of single-pass perforated absorbing muffler with Msc.Actran. In the first approach, the sound absorbing material is modelled as rigid porous material which is one of the material models available in Msc.Actran library. In this approach, the flexibility of the material is neglected. Porous materials are defined by two sets of parameters in Msc.Actran, namely, acoustic parameters and poro-mechanical parameters. The fluid density is the only necessary acoustic parameter for a porous material; however poro-mechanical properties consist of porosity, resistivity, fluid bulk modulus and tortuosity. Fluid bulk modulus describes the compressibility of the fluid within the pores of the material. On the other hand, tortuosity describes the complexity of the path that a fluid particle must follow to proceed from one point to another point. However, there is no information for these two parameters in Selamet's study; therefore, these are not used in the first modelling approach. Moreover, the

perforated duct is modelled by transfer admittance boundary condition in which Mechel's formula is used for calculation of perforation impedance in the first approach. In the second modelling approach, sound absorbing material is modelled as an acoustic material which is described by complex acoustic impedance and the wave number as given in the study by Selamet et al. [37]. On the other hand, the perforated duct is modelled by transfer admittance boundary condition in which the impedance for the perforation is calculated as in Equation (4.12). The acoustic impedance of perforation in contact with air-fibrous material is considered in the second model, whereas, acoustic impedance of perforation in contact with air-air is considered in the first model.

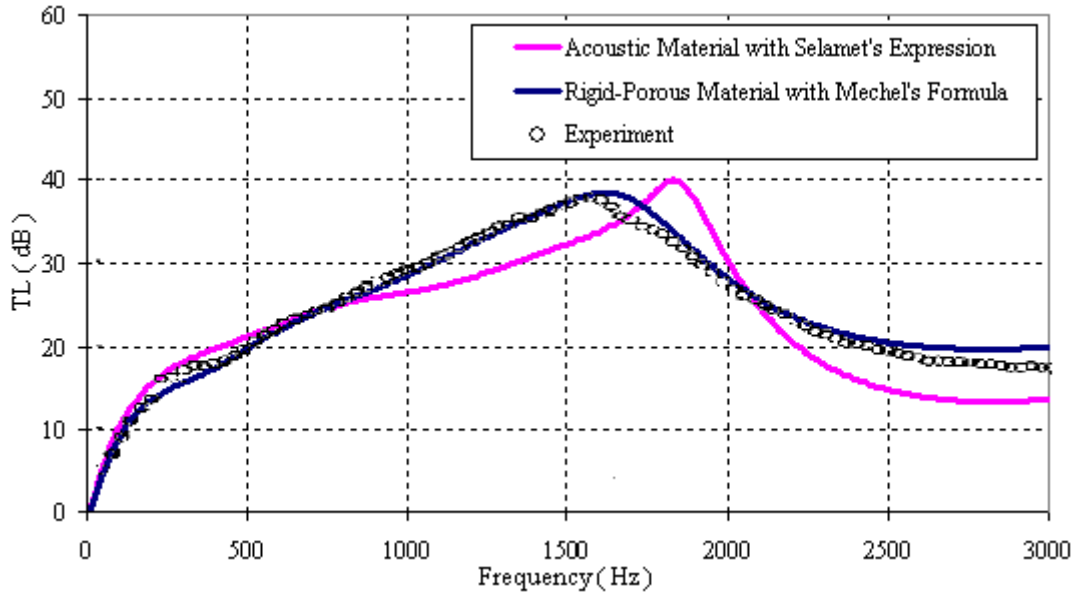

Figure 4.10 – Comparison of the results obtained by two modelling approaches with experiment for single-pass perforated absorbing muffler

Transmission losses of the single-pass perforated muffler are calculated by Msc.Actran for the two modelling approaches. The same FE model, which consists of 7378 hexahedral elements and 6270 nodes, is used for the both models. In Figure

4.10, the numerical results for the prediction of transmission losses are presented and compared with the experimental result given in the study by Selamet et al. [37]. .A reasonable agreement with the experimental result is obtained for the first approach in which sound absorbing material is modelled with acoustic material with the complex characteristic impedance and wave number. The prediction from the first modelling approach matches closely the experimental result throughout the frequency range of interest. However, it is observed that there is a slight difference between the experimental result and numerical result for the second approach. This difference may be due to the lack of the poro-mechanical properties of sound absorbing material. Despite this, the prediction of the transmission loss obtained from the second modelling approach in which rigid porous material with Mechel's formula is used, captures the trend of the experimental result with a slight shift in the peak frequency. Therefore, this modelling approach is used throughout the study since there is no experimental data for the complex speed of sound and wave number for the sound absorbing material.

The sufficiency of total number of elements used in the finite element method is confirmed by convergence test. Therefore, additional analysis by using 35156 hexahedral elements and 31263 nodes has been performed for both the first and the second modelling approaches. Transmission loss results are compared in Figure 4.11 and Figure 4.12, respectively. It can be observed that there is nearly no difference between the results obtained from the models with different mesh sizes at the frequency range of interest. Hence, it is confirmed that sufficient number of elements has been used in the finite element models for the single-pass perforated muffler.

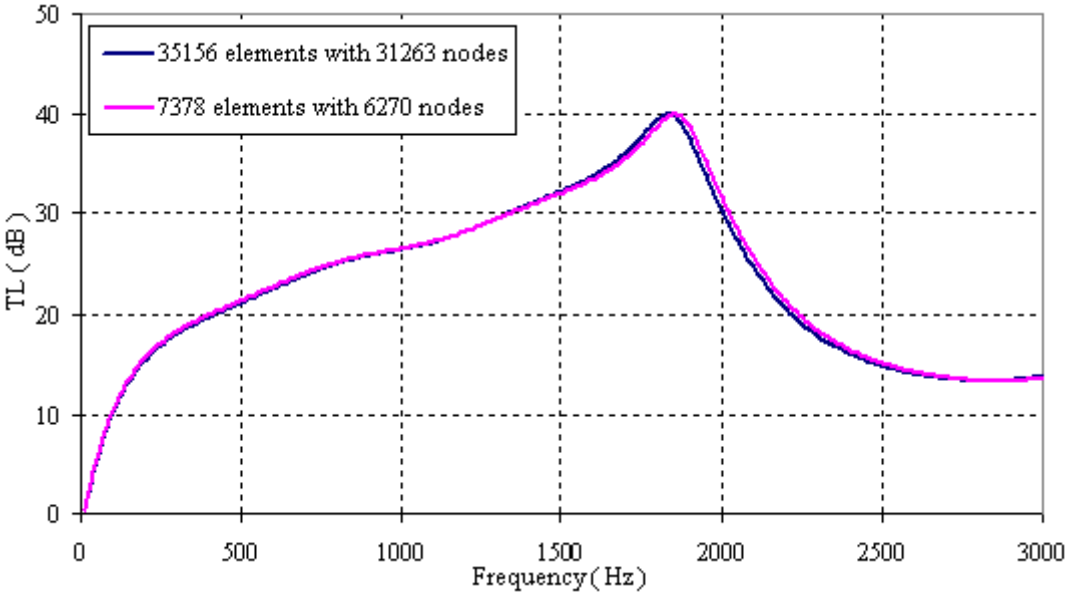

Figure 4.11 – Transmission loss results for the first modelling approach of single-pass perforated absorbing muffler

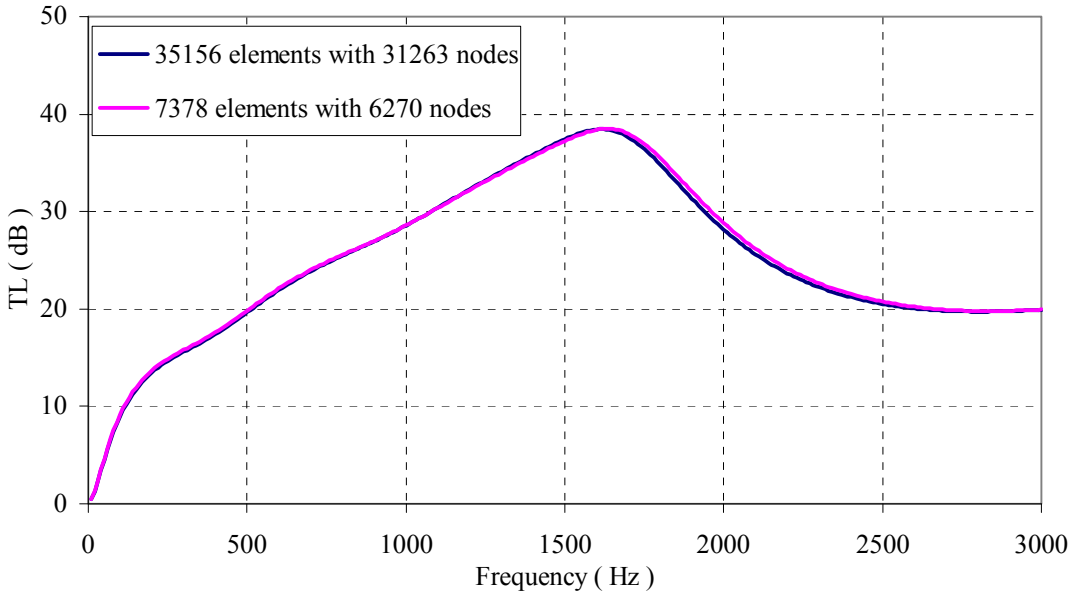

Figure 4.12 – Transmission loss results for the second modelling approach of single-pass perforated absorbing muffler

CHAPTER 5

TRANSMISSION LOSS MEASUREMENT

In this chapter, transmission loss measurement methods that have been frequently used in literature are explained; namely, Chung-Blaser method, two-source method and two-load method. Derivations of mathematical expressions used in these methods are also given. Furthermore, the chapter covers the experimental test setup developed for transmission loss measurements. In the test setup, these methods are applied to determine the transmission loss of a single expansion chamber with extended inlet/outlet. Experimental results are compared with 1-D analytical solution obtained by transfer matrix method. FEM prediction for the transmission loss by Msc.Actran is also presented.

5.1 Transmission Loss Measurement Techniques

5.1.1 Chung-Blaser Method [26]

In Chung-Blaser method, a stationary random acoustic plane wave is decomposed into its incident and reflected components, and complex reflection coefficient is determined using a transfer function relation between acoustic pressures at two locations on the tube. Transmission loss of a muffler is then evaluated from the complex reflection coefficient. The test setup is shown in Figure 5.1.

The sound pressure P_1 and P_2 in these two-microphone position are composed of incident and reflected plane waves as:

$$P_1 = A + B \tag{5.1}$$

$$P_2 = Ae^{jks} + Be^{-jks} \tag{5.2}$$

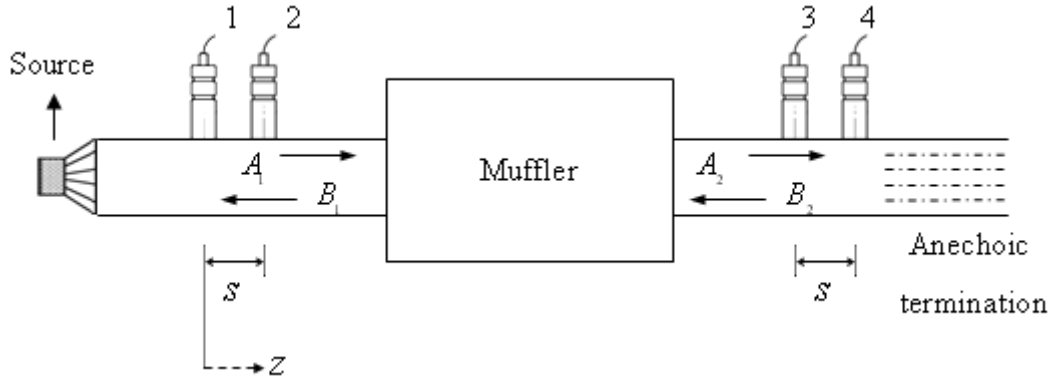

Figure 5.1 – Measurement setup of Chung-Blaser method

The reflection coefficient, which is the ratio of amplitude of the reflected wave to that of the incident wave at the first microphone position at the upstream tube, is

$$r_u = \frac{B}{A} \tag{5.3}$$

Therefore, the transfer function H_{12} can be obtained as:

$$H_{12} = \frac{P_2}{P_1} = \frac{1 + r_u}{e^{jks} + r_u e^{-jks}} \tag{5.4}$$

The reflection coefficient at the upstream tube, r_u, can be obtained transposing Equation (5.4) as:

$$r_u = \frac{H_{12} - e^{-jks}}{e^{jks} - H_{12}} \tag{5.5}$$

Similarly, the reflection coefficient at the third microphone position at the downstream tube, r_d, can be obtained as:

$$r_d = \frac{H_{34} - e^{-jks}}{e^{jks} - H_{34}} \tag{5.6}$$

The sound power incident on the muffler and the sound power transmitted through the muffler can be written as:

$$W_i = \frac{S_{11} A_u}{(\rho c)\left|1 + r_u\right|^2} \tag{5.7}$$

$$W_t = \frac{S_{33} A_d}{(\rho c)\left|1 + r_d\right|^2} \tag{5.8}$$

where S_{11}, S_{33} are the auto-spectra of the measured sound pressures and A_u, A_d are the cross-sectional area at the upstream measurement location.

Hence, the transmission loss can be calculated as:

$$\begin{aligned} TL &= 10\log\left(\frac{W_i}{W_t}\right) \\ &= 20\log\left|\frac{e^{jks} - H_{12}}{e^{jks} - H_{34}}\right| + 20\log\left|\frac{S_{11}}{S_{33}}\right| + 10\log\left(\frac{A_u}{A_d}\right) \end{aligned} \tag{5.9}$$

5.1.2 Two-Source Method [28]

Two-source method is based on transfer matrix method. The four-pole parameters of the muffler is determined by measuring the acoustic pressure at the four fixed locations, namely, two upstream and two downstream in two test configurations as shown in Figure 5.2.

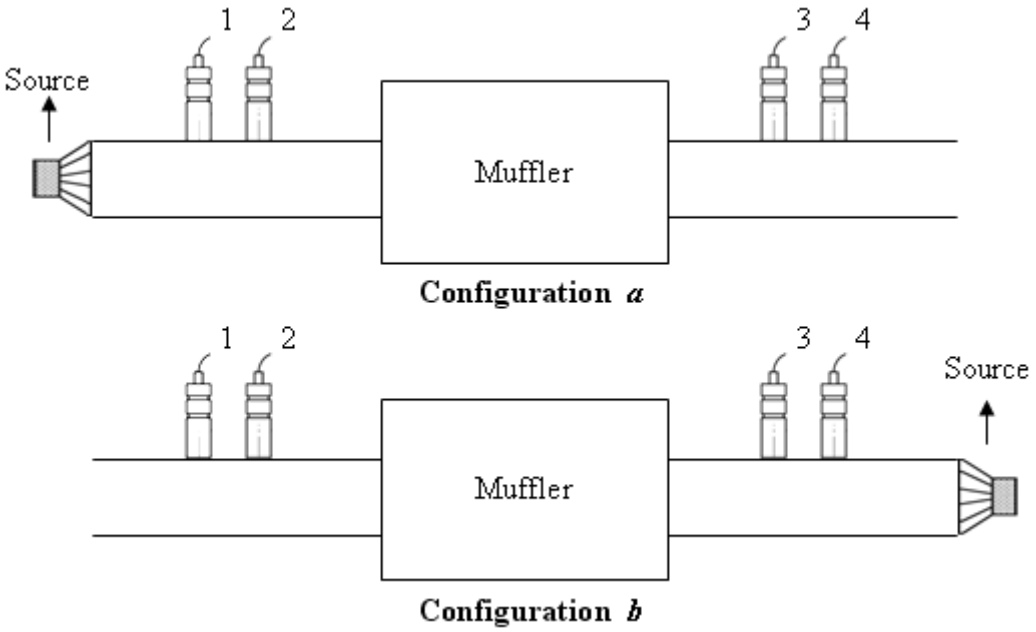

Figure 5.2 – Measurement setup of two-source method

Through Equation (3.8), the muffler can be modelled by its four-pole parameters as below:

$$\begin{bmatrix} P_i \\ v_i \end{bmatrix} = \begin{bmatrix} A_{ij} & B_{ij} \\ C_{ij} & D_{ij} \end{bmatrix} \begin{bmatrix} P_j \\ v_j \end{bmatrix} \tag{5.10}$$

where P_i and P_j are the sound pressures; v_i and v_j are the acoustic mass velocity at the inlet and outlet, respectively, and A_{ij}, B_{ij}, C_{ij} and D_{ij} are the four-pole parameters of the acoustical elements.

One can readily obtain four-pole equations for the straight tube elements between microphones 1-2 and 3-4. These can be expressed as

$$\begin{bmatrix} P_1 \\ v_1 \end{bmatrix} = \begin{bmatrix} A_{12} & B_{12} \\ C_{12} & D_{12} \end{bmatrix} \begin{bmatrix} P_2 \\ v_2 \end{bmatrix} \tag{5.11}$$

$$\begin{bmatrix} P_3 \\ v_3 \end{bmatrix} = \begin{bmatrix} A_{34} & B_{34} \\ C_{34} & D_{34} \end{bmatrix} \begin{bmatrix} P_4 \\ v_4 \end{bmatrix} \tag{5.12}$$

where the transfer matrices are found by Equation (3.16) as:

$$\begin{bmatrix} A_{12} & B_{12} \\ C_{12} & D_{12} \end{bmatrix} = \begin{bmatrix} \cos(kl_{12}) & jY_u \sin(kl_{12}) \\ j\sin(kl_{12})/Y_u & \cos(kl_{12}) \end{bmatrix} \tag{5.13}$$

$$\begin{bmatrix} A_{34} & B_{34} \\ C_{34} & D_{34} \end{bmatrix} = \begin{bmatrix} \cos(kl_{34}) & jY_d \sin(kl_{34}) \\ j\sin(kl_{34})/Y_d & \cos(kl_{34}) \end{bmatrix} \tag{5.14}$$

In Equation (5.13) and Equation (5.14), l_{12} and l_{34} are the microphone spacing for the corresponding elements 1-2 and 3-4. Y_d and Y_u are the characteristic impedance in downstream and upstream side of the muffler, respectively. Similarly, the four-pole equation for element 2-3 which includes the muffler can be expressed as:

$$\begin{bmatrix} P_{2a} \\ v_{2a} \end{bmatrix} = \begin{bmatrix} A_{23} & B_{23} \\ C_{23} & D_{23} \end{bmatrix} \begin{bmatrix} P_{3a} \\ v_{3a} \end{bmatrix} \tag{5.15}$$

where the subscript ‘a’ refers to “Configuration a” in Figure 5.2 above. Combining equations from (5.11) to (5.15) yields

$$\begin{bmatrix} P_{2a} \\ \frac{1}{B_{12}}(P_{1a} - A_{12}P_{2a}) \end{bmatrix} = \begin{bmatrix} A_{23} & B_{23} \\ C_{23} & D_{23} \end{bmatrix} \begin{bmatrix} P_{3a} \\ \frac{D_{34}}{B_{34}}P_{3a} + (C_{34} - \frac{D_{34}A_{34}}{B_{34}})P_{4a} \end{bmatrix} \quad (5.16)$$

One can see in Equation (5.16) that there are four unknowns which are the four-pole parameters between the acoustical element 2-3, namely A_{23}, B_{23}, C_{23} and D_{23}. However, there are only two equations available. In order to obtain two additional equations, the sound source is shifted to the other end and the four-pole parameters of element 3-2 can be evaluated. For configuration b, one can then write

$$\begin{bmatrix} P_{3b} \\ -v_{3b} \end{bmatrix} = \begin{bmatrix} A_{23} & B_{23} \\ C_{23} & D_{23} \end{bmatrix}^{-1} \begin{bmatrix} P_{2b} \\ -v_{2b} \end{bmatrix} = \frac{1}{\Delta} \begin{bmatrix} D_{23} & B_{23} \\ C_{23} & A_{23} \end{bmatrix} \begin{bmatrix} P_{2b} \\ -v_{2b} \end{bmatrix} \quad (5.17)$$

where Δ is the determinant of the matrix,

$$\Delta = A_{23}D_{23} - B_{23}C_{23} \quad (5.18)$$

The minus sign in Equation (5.17) is due to the change of the velocity direction in Configuration b. Using the same approach as before, one can obtain another four-pole equation given as:

$$\begin{bmatrix} P_{3b} \\ \frac{-1}{B_{34}}(\Delta_{34}P_{4b} - D_{34}P_{4a}) \end{bmatrix} = \frac{1}{\Delta} \begin{bmatrix} D_{23} & B_{23} \\ C_{23} & A_{23} \end{bmatrix} \begin{bmatrix} P_{2a} \\ (\frac{C_{12}}{\Delta_{12}} - \frac{A_{12}D_{12}}{\Delta_{12}B_{12}})P_{1b} - \frac{A_{12}}{B_{12}}P_{2b} \end{bmatrix} \quad (5.19)$$

where the determinants Δ_{12} and Δ_{34} are

$$\Delta_{12} = A_{12}D_{12} - B_{12}C_{12} \tag{5.20}$$

$$\Delta_{34} = A_{34}D_{34} - B_{34}C_{34} \tag{5.21}$$

Also, note that $\Delta_{12} = 1$ and $\Delta_{34} = 1$ from Equation (3.16).

Using both Equation (5.16) and Equation (5.19), the four-pole parameters can be written in terms of transfer functions as:

$$A_{23} = \frac{(H_{32,a}H_{34,b} - H_{32,b}H_{34,a}) + D_{43}(H_{32,b} - H_{32,a})}{(H_{34,b} - H_{34,a})} \tag{5.22}$$

$$B_{23} = \frac{B_{34}(H_{32,a} - H_{32,b})}{(H_{34,b} - H_{34,a})} \tag{5.23}$$

$$C_{23} = \frac{(H_{31,a} - A_{12}H_{32,a})(H_{34,b} - D_{34}) - (H_{31,b} - A_{12}H_{32,b})(H_{34,a} - D_{34})}{B_{12}(H_{34,b} - H_{34,a})} \tag{5.24}$$

$$D_{23} = \frac{(H_{31,a} - H_{31,b}) + A_{12}(H_{32,b} - H_{32,a})}{B_{12}(H_{34,b} - H_{34,a})} B_{34} \tag{5.25}$$

Since the four-pole parameters of the muffler elements are obtained, the transmission loss of the muffler can be calculated by Equation (3.25) as:

$$TL = 20\log_{10}\left\{\frac{1}{2}\left|A_{23} + \frac{B_{23}}{Y_d} + Y_u C_{23} + (\frac{Y_d}{Y_u})D_{23}\right|\right\} + 10\log_{10}(\frac{S_u}{S_d}) \tag{5.26}$$

5.1.3 Two-Load Method [38]

Two-load method is also based on transfer matrix method. Instead of transfer matrix relation between acoustic pressure and acoustic mass velocity at the upstream and downstream of the muffler, the relation is expressed between incident and reflected wave at the upstream and downstream side of the muffler as shown in Figure 5.3. Transfer matrix relation can be written as:

$$\begin{bmatrix} A_1 \\ B_1 \end{bmatrix} = \begin{bmatrix} \alpha & \beta \\ \gamma & \delta \end{bmatrix} \begin{bmatrix} A_2 \\ B_2 \end{bmatrix} \tag{5.27}$$

where A_1 and B_1 are incident and reflected waves at the downstream of the muffler, A_2 and B_2 are incident and reflected waves at the upstream of the muffler.

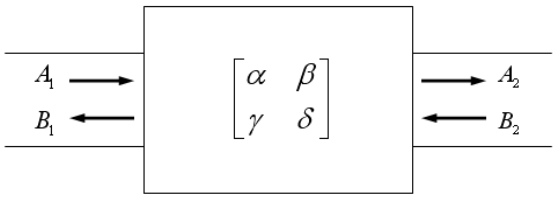

Figure 5.3 –Transfer matrix relation between incident and reflected waves

By definition, transmission loss can then be expressed as:

$$TL = 20\log|\alpha| \tag{5.28}$$

where α can be defined as the ratio of the amplitude of incident wave at the downstream of the muffler to the amplitude of the incident wave at the upstream side

of the muffler for the hypothetical case of amplitude of the reflected wave at the upstream is zero.

Two-load method involves measurements with two different terminations as shown in Figure 5.4. Open ended and closed ended terminations are used to obtain two different loads. Therefore, incident and reflected waves can be expressed by transfer matrix for open and closed configurations as:

$$\begin{bmatrix} A_{1C} \\ B_{1C} \end{bmatrix} = \begin{bmatrix} \alpha & \beta \\ \gamma & \delta \end{bmatrix} \begin{bmatrix} A_{2C} \\ A_{2C} \end{bmatrix} \tag{5.29}$$

$$\begin{bmatrix} A_{1O} \\ B_{1O} \end{bmatrix} = \begin{bmatrix} \alpha & \beta \\ \gamma & \delta \end{bmatrix} \begin{bmatrix} A_{2O} \\ B_{2O} \end{bmatrix} \tag{5.30}$$

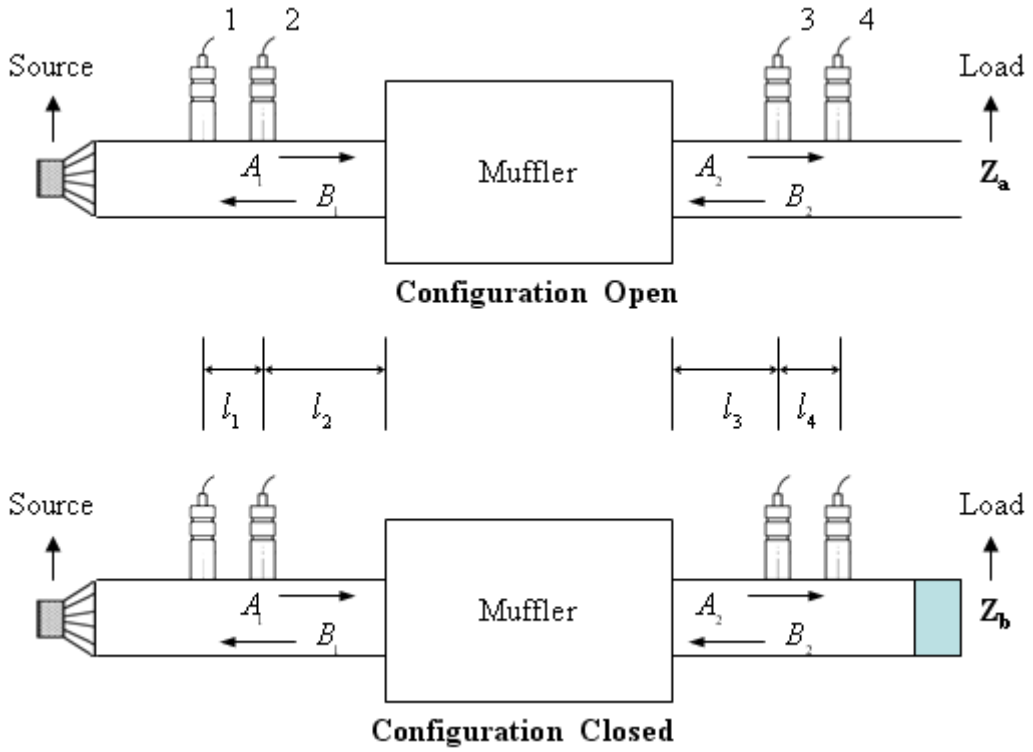

Figure 5.4 – Measurement setup of two-load method

By using Equation (5.29) and Equation (5.30), α can be found as:

$$\alpha = \frac{A_{1O}B_{2C} - A_{1C}B_{2O}}{A_{2O}B_{2C} - A_{2C}B_{2O}} \tag{5.31}$$

The acoustic pressure at the measurement points of the test setup can be expressed in terms of incident and reflected waves as:

$$P_1 = A_1 e^{jk(l_1+l_2)} + B_1 e^{-jk(l_1+l_2)} \tag{5.32}$$

$$P_2 = A_1 e^{jkl_2} + B_1 e^{-jkl_2} \tag{5.33}$$

$$P_3 = A_2 e^{-jkl_3} + B_2 e^{-jkl_3} \tag{5.34}$$

$$P_4 = A_2 e^{-jk(l_3+l_4)} + B_2 e^{-jk(l_3+l_4)} \tag{5.35}$$

The incident and reflected waves at the downstream of the muffler is obtained by using Equation (5.32) and Equation (5.33) as

$$A_1 = \frac{-j}{2}\frac{P_1 - P_2 e^{-jkl_1}}{\sin(kl_1)} e^{-jkl_2} \tag{5.36}$$

$$B_1 = \frac{j}{2}\frac{P_1 - P_2 e^{jkl_1}}{\sin(kl_1)} e^{jkl_2} \tag{5.37}$$

The incident and reflected waves at the upstream of the muffler are obtained by using Equation (5.34) and Equation (5.35) as:

$$A_2 = \frac{j}{2}\frac{P_4 - P_3 e^{jkl_4}}{\sin(kl_4)} e^{jkl_3} \tag{5.38}$$

$$B_2 = \frac{-j}{2}\frac{P_4 - P_3 e^{-jkl_4}}{\sin(kl_4)} e^{-jkl_3} \tag{5.39}$$

These incident and reflected waves can also be expressed in terms of auto and cross spectra as:

$$A_1 P_1^* = \frac{-j}{2}\frac{S_{11} - S_{12} e^{-jkl_1}}{\sin(kl_1)} e^{-jkl_2} \tag{5.40}$$

$$B_1 P_1^* = \frac{j}{2}\frac{S_{11} - S_{12} e^{jkl_1}}{\sin(kl_1)} e^{jkl_2} \tag{5.41}$$

$$A_2 P_1^* = \frac{j}{2}\frac{S_{14} - S_{13} e^{jkl_4}}{\sin(kl_4)} e^{jkl_3} \tag{5.42}$$

$$B_2 P_1^* = \frac{-j}{2}\frac{S_{14} - S_{13} e^{-jkl_4}}{\sin(kl_4)} e^{-jkl_3} \tag{5.43}$$

Therefore, the measured data are the auto-spectrum of the signal at the first microphone location, S_{11}, and the cross-spectrum between the first and the other microphones which are S_{12}, S_{13}, S_{14}. Finally, transmission loss can be expressed as:

$$TL = 20\log\left|\frac{\{A_{1O}P_{1O}^*\}\{B_{2C}P_{1C}^*\} - \{A_{1C}P_{1C}^*\}\{B_{2O}P_{1O}^*\}}{\{A_{2O}P_{1O}^*\}\{B_{2C}P_{1C}^*\} - \{A_{2C}P_{1C}^*\}\{B_{2O}P_{1O}^*\}}\right| \tag{5.44}$$

5.2 Transmission Loss Measurement Setup

The experimental setup designed for the transmission loss measurement mainly consists of an impedance tube, four microphones, a sound source and a digital frequency analysis system. The experimental setup is shown schematically in Figure 5.5.

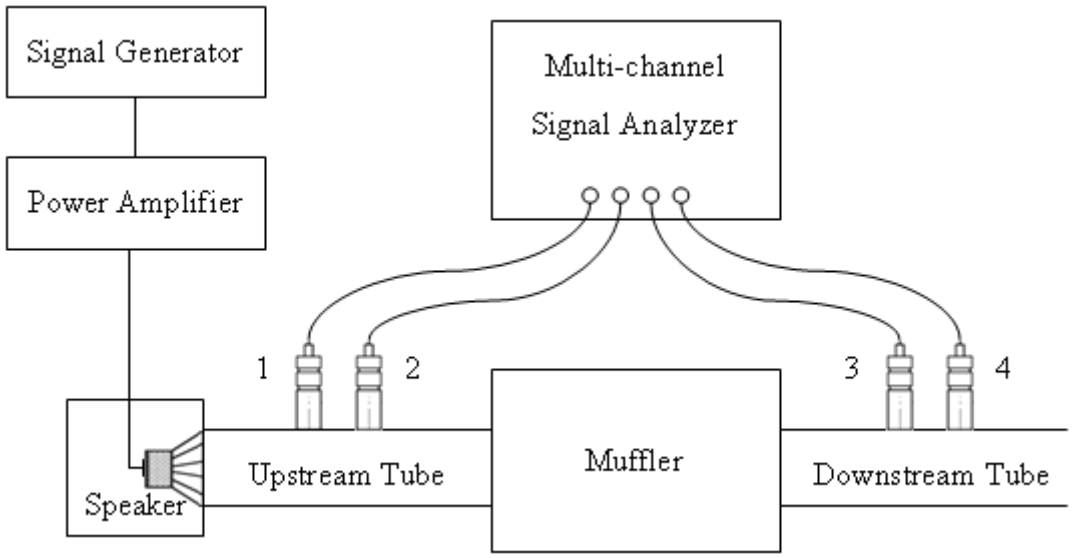

Figure 5.5 – Transmission loss measurement setup

5.2.1 Test Equipments

The muffler is mounted between upstream and downstream tubes as shown in Figure 5.5. A loudspeaker contained in an insulating box is located at the opposite end of the tube from muffler. A loudspeaker of 2W rated power is used as a sound source in the test setup. The loudspeaker is driven by a signal generator, which generates a stationary random signal. In the test setup, Brüel & Kjaer type 1405 noise generator (serial number: 1746080), is used as a signal generator and generates white noise as excitation signal. To amplify the signal coming from the noise generator, Marantz

type PM 4001 integrated amplifier (serial number: MZ000530000604) is used in the measurement setup. The microphones, G.R.A.S. type 40AE ½ inch condenser microphones (serial numbers: 86571, 86577, 86679, 86680) are mounted to the surface of the upstream and downstream tubes two by two. Finally, the microphones are connected to multi-channel signal analyzer, which is Sinus Soundbook measuring system (serial number: 7BKCBB81615). Signal analyzer is used to determine auto-spectra, cross-spectra and transfer function of microphone signals.

5.2.2 Specifications of the Test Setup

The measurement points should be in the plane wave field in the test setup. Therefore, the impedance tube should be long enough to allow plane wave propagation between the loudspeaker and the muffler. However; sound waves produced by loudspeakers vary from plane waves to other types such as spherical etc. depending on the frequency and distance from the speaker. The non-plane waves usually will subside at a distance equivalent to three tube diameters from the source Therefore, the distance more than three tube diameters is recommended between the loudspeaker and the nearest microphone [39].

Measurements in the test setup are valid only between upper and lower working frequencies of the impedance tube. The upper working frequencies should be chosen to avoid the occurrence of non-plane wave mode propagation as in Equation (5.45) [39].

$$f_u = 0.58\frac{c}{D} \tag{5.45}$$

where D is the diameter of the impedance tube.

The lower frequency limit depends on the spacing of the microphones and the accuracy of the analysis system. It is recommended that the microphone spacing must exceed one percent of the wavelength corresponding to the lower frequency of interest [40]. Therefore, the lower frequency limit, f_l , can be determined by

$$f_l = 0.01\frac{c}{s} \tag{5.46}$$

Spacing between the microphones is also important for the accuracy of the measurements. A large spacing between microphones enhances the accuracy of the measurements; however, the microphone spacing must be less than the shortest half wavelength of interest. It is recommended that the maximum microphone spacing is eighty percent of $c/2f_u$ [40]. Therefore, microphone spacing, s, is determined in the test setup by the following equation:

$$s = 0.4\frac{c}{f_u} \tag{5.47}$$

5.2.3 Calibration of the Microphones

Since the transfer function is a complex ratio of the acoustic pressure responses, any mismatch in the amplitude or phase responses of the two microphone systems will affect the accuracy of the transfer function measurement. The following sequence of measurements and computations provides a means for correcting the measured transfer function data in both measurement channels [39]. This method is repeated for each pair of microphones in turn yielding relative microphone calibration data.

1. Place a highly absorptive material in the tube to prevent strong acoustic reflections and to obtain the most accurate correction factor possible.

2. Place the microphones in Configuration I as in Figure 5.6 and store the transfer function $H_{12}^{\ I}$.

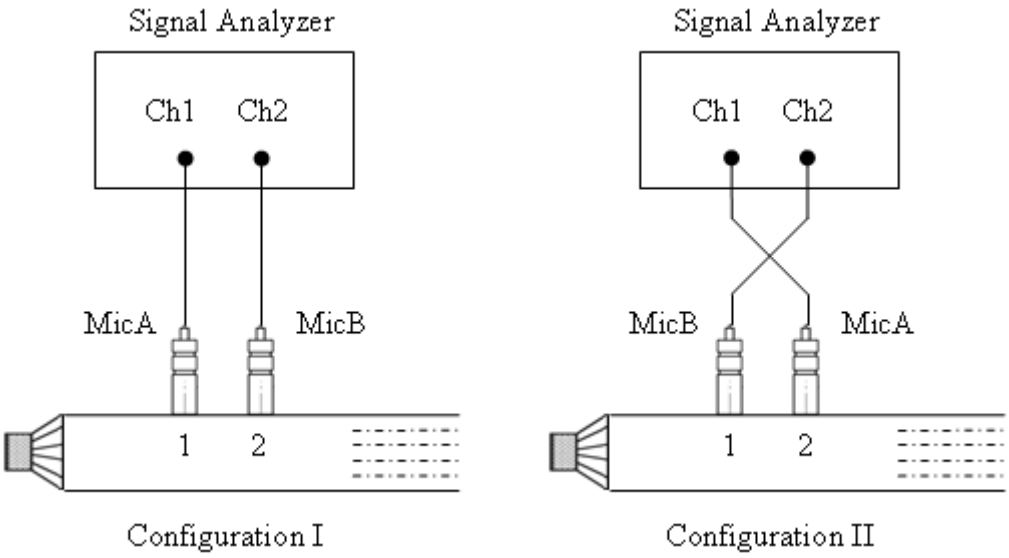

Figure 5.6 – Configurations for microphone calibration

3. Interchange the microphones A and B in such away that microphone A in Configuration II occupies the precise location that microphone B in Configuration I.
4. Measure the transfer function $H_{12}^{\ II}$ and calculate the calibration factor as:

$$H_c = \left(H_{12}^{\ I} / H_{12}^{\ II} \right)^{1/2} \tag{5.48}$$

5. For the transmission loss measurement, place the microphones in configuration I, and measure the transfer function $\hat{H}_{12}$.
6. Correct the microphone responses for mismatch in using

$$H_{12} = \hat{H}_{12} / H_c \tag{5.49}$$

where $\hat{H}_{12}$ the uncorrected transfer is function and H_{12} is the corrected transfer function.

5.3 Validation of Transmission Loss Measurement Setup

In order to verify the experimental test setup, transmission loss of a single expansion chamber with extended inlet/outlet is determined with three different methods, namely, Chung-Blaser method, two-source method and two-load method. The schematic of the single expansion chamber with extended inlet/outlet and the experimental setup are shown in Figure 5.7 and Figure 5.8, respectively. The results are compared with 1-D analytical solution obtained by TMM and transmission loss prediction by Msc.Actran is also given.

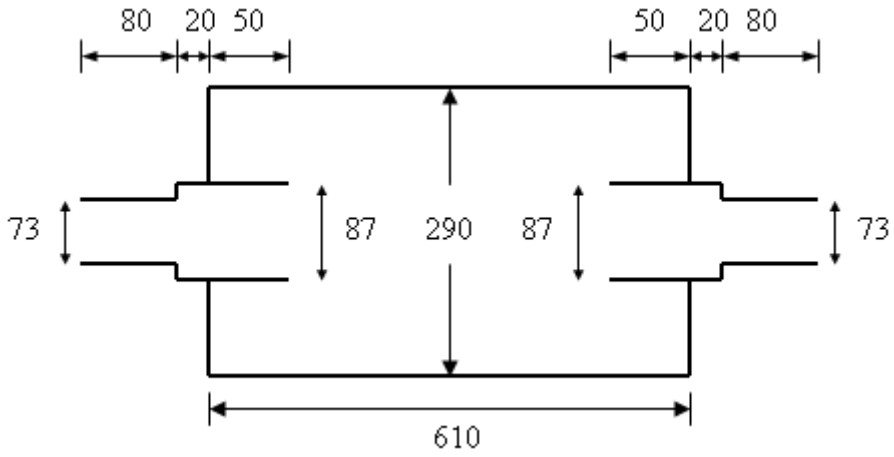

Figure 5.7 – Single expansion chamber with extended inlet/outlet
(Dimensions are given in mm)

Experiments are carried out using all three-transmission loss measurement techniques in the same test setup in the absence of mean flow at room temperature. An anechoic termination whose absorption coefficient is about 0.95 over 100 Hz-

5000 Hz frequency range is used in the measurements. The loudspeaker is excited with a band-limited white noise up to 20 kHz. Spectral analysis is carried on the Soundbook measurement system with the following parameters: Sample record length 40.96 s, Number of averages: 128, Sampling frequency: 6400 Hz, Window type: Hanning. The room temperature is also measured to calculate speed of sound. The microphone spacing, $s = 50$ mm is used for the upstream and downstream impedance tubes. Therefore, all the results of measurements presented below are valid for frequencies between about 70 Hz and 2650 Hz, that is, only plane waves are propagating in the impedance tubes between these frequencies.

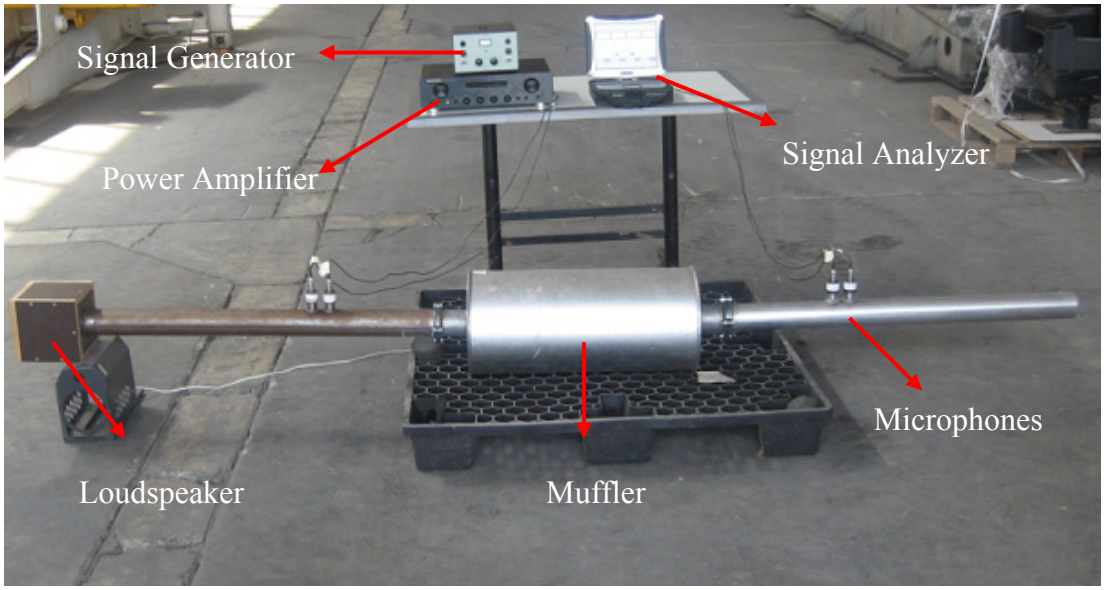

Figure 5.8 – Single expansion chamber with extended inlet/outlet

The microphones are calibrated in order to compensate the phase and amplitude mismatch among the four microphones by following the procedure explained in 5.2.3. The amplitude and phase difference characteristics between the microphones are shown in Figure 5.9 and 5.10, respectively. It can be observed that there is nearly no amplitude mismatch between the microphones. Besides, the phase difference between the microphones is less than 1 degree.

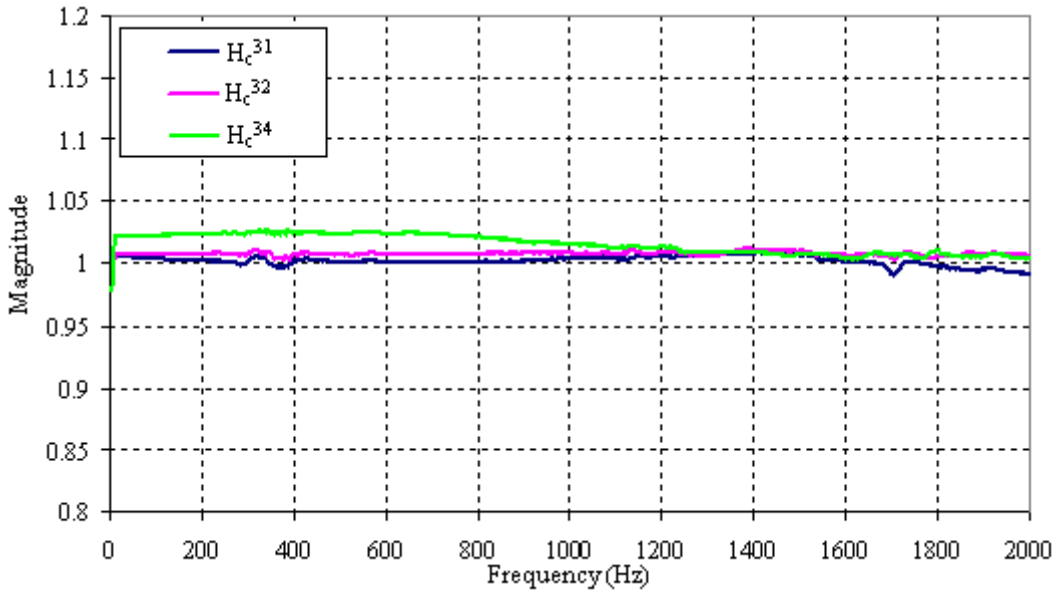

Figure 5.9 – Modulus of the calibration factor between the microphones

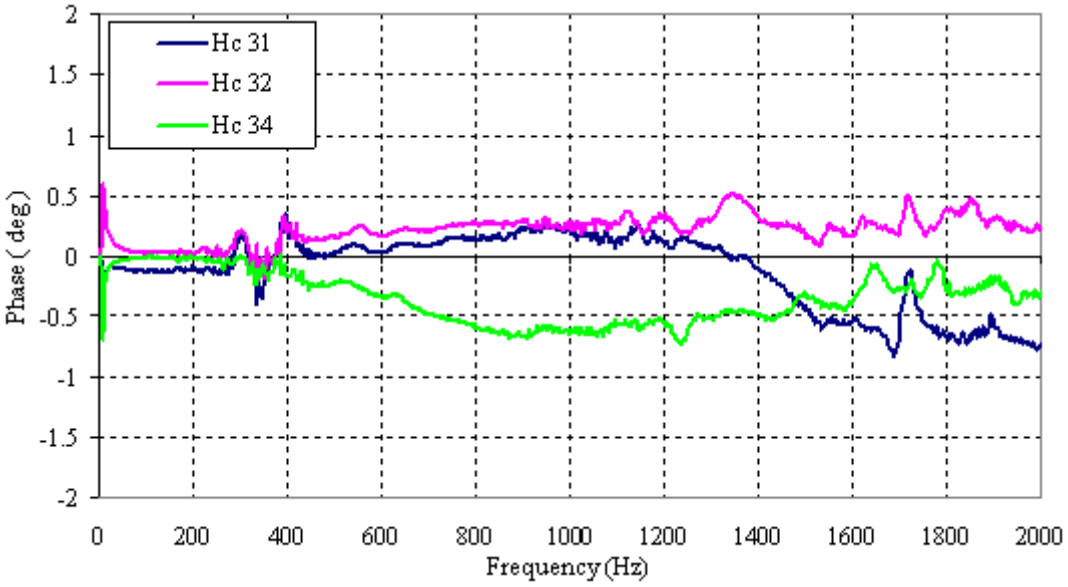

Figure 5.10 – Phase angle of the calibration factor between the microphones

In transmission loss measurement, plane waves are tried to be generated in the upstream tube. However, one or more of higher order modes get cut on in the chamber, even though the inlet and outlet ducts may permit plane waves. Therefore,

cut-on frequencies for the higher order modes in expansion chamber are calculated by using Equation (3.2) and plotted as vertical lines in figures showing the results of the measurement. The cut-on frequencies of the expansion chamber are about 700 Hz for the (1, 0) mode, 1165 Hz for the (2, 0) mode and 1460 Hz for the (0, 1) mode.

In Figure 5.11, the experimental result by Chung-Blaser method is compared with the 1-D analytical result and FEA result of Msc.Actran for single expansion chamber with extended inlet/outlet. It can be observed from the experimental result that there is a combination of domes of a simple expansion chamber and the resonant peak due to the extended inlet/outlet.

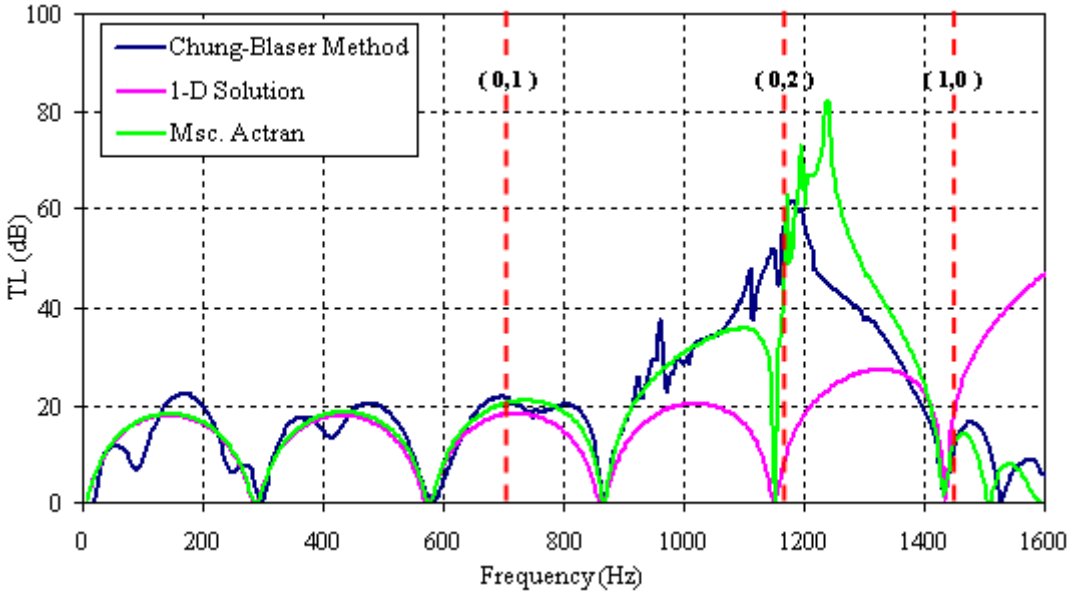

Figure 5.11 – Comparison of experimental result obtained by Chung-Blaser method with 1-D solution and Msc.Actran prediction

Below about 700 Hz, which is also the cut-off frequency for the plane propagation in the chamber, dome-like behaviour of single expansion chamber in the plane wave region can be clearly observed. Minimum transmission loss occurs at the frequencies where the length of the chamber equals integer multiple of a half-wavelength and

maximum transmission loss occur at the frequencies where the length of the chamber equals odd multiples of a quarter-wavelength. In plane wave region, Msc.Actran prediction for transmission loss match closely the 1-D solution by TMM, however, the experimental result by using Chung-Blaser method shows some discrepancies in the domes. At higher frequencies, the result of 1-D solution deviates from the experimental and FEA results as expected, since 1-D solution excludes the effect of higher order modes. However, FEA result shows fairly good agreements with the experimental result for this region.

Figure 5.12 shows the comparison of the experimental result by two-source method with 1-D analytical result and FEA result of Msc.Actran. Although the experimental result by two-source method captures the trend of the dome-like behaviour of single expansion camber, there is a significant difference in magnitude of transmission loss.

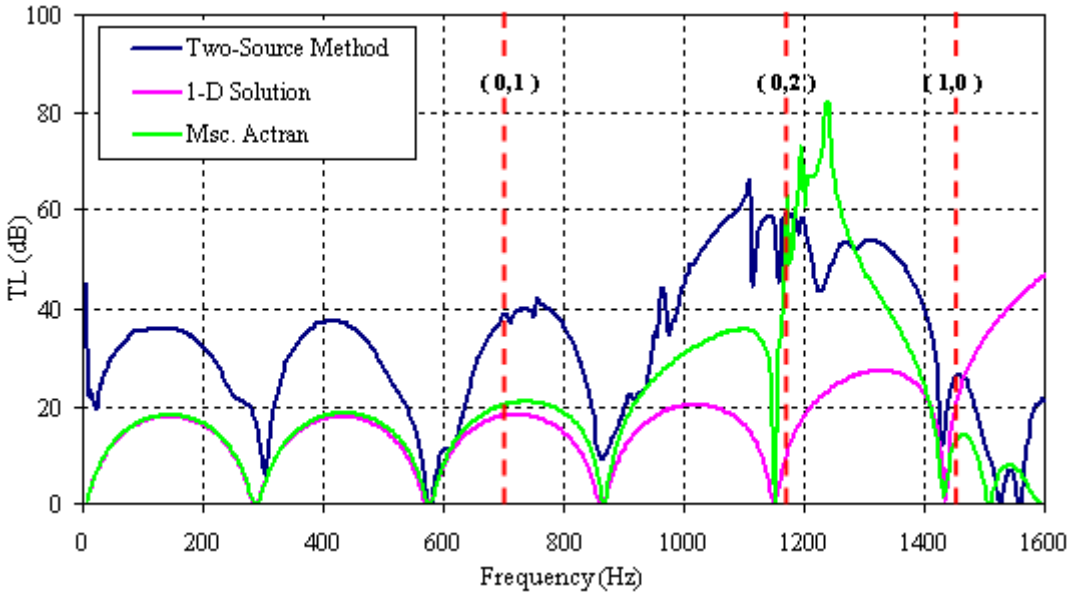

Figure 5.12 – Comparison of experimental result obtained by two-source method with 1-D solution and Msc.Actran prediction

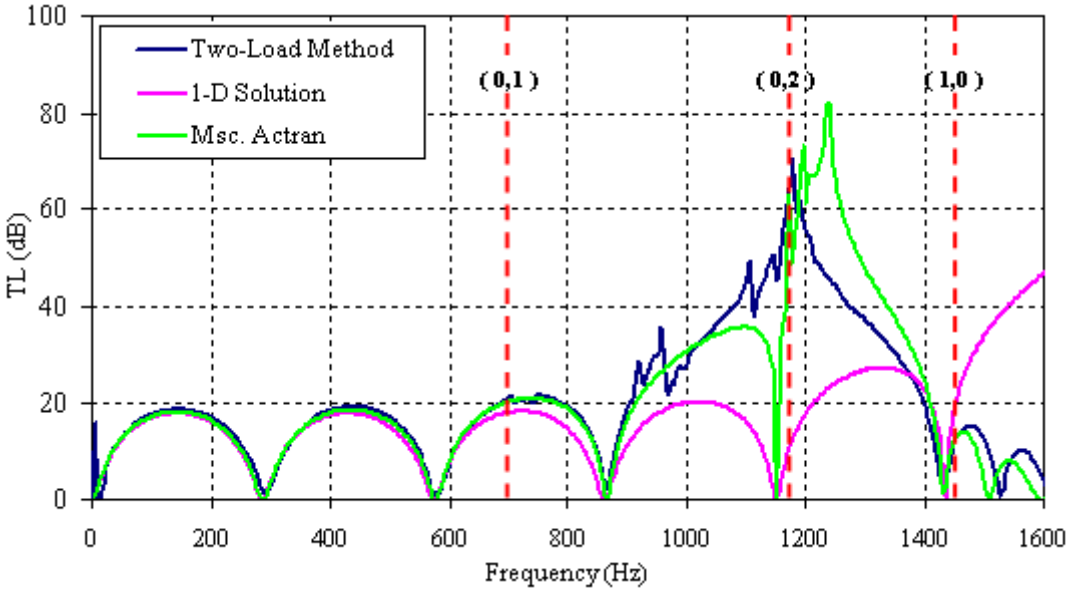

Figure 5.13 – Comparison of experimental result obtained by two-load method with 1-D solution and Msc.Actran prediction

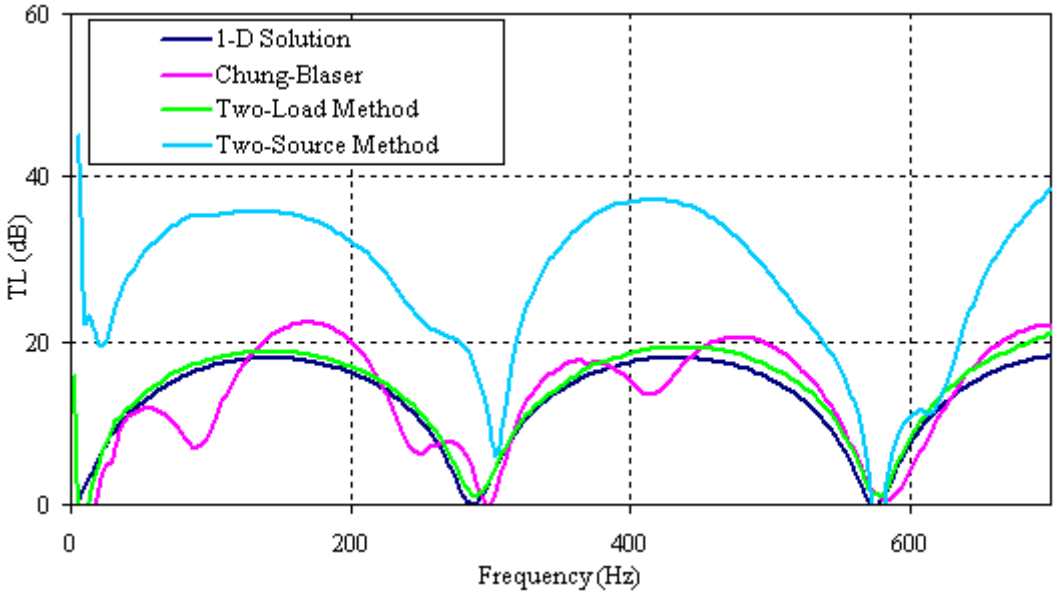

Figure 5.14 – Comparisons of the experimental methods with 1-D Solution

The two-load experimental method and 1-D analytical prediction yield nearly identical results in the plane wave region, and both also agree with the Msc.Actran results as shown in Figure 5.13. There is also a good agreement between numerical and experimental result in higher frequencies. Some differences between the results may be due to neglected viscous effects in the analysis and some minor geometrical differences in the prototype muffler.

Figure 5.14 shows the transmission loss comparison of the three experimental methods used in the test setup with 1-D analytical method. It can be easily observed that transmission loss result obtained by two-load method shows the best agreement with 1-D solution for the designed experimental setup. Hence, it has been decided that the measurement of the transmission loss of the muffler of interest will be conducted in the developed experimental setup with two-load method.

CHAPTER 6

CASE STUDY

Acoustical performance of the muffler used on HMK 200W-3 wheeled excavator, manufactured by Hidromek Inc. is investigated both experimental and numerical means. The transmission loss of the muffler of interest is calculated by performing FEA with Msc.Actran. The transmission loss is also determined in the developed experimental setup with two-load method. After the comparison of numerical and experimental results, the effect of temperature and flow on the transmission loss is investigated numerically.

6.1 Description of the Muffler

Structure of the muffler under study is shown schematically in Figure 6.1. The muffler has three partitions, which divide cylindrical drum-shaped body into four chambers. The exhaust gases coming from the engine enters the first chamber of the muffler via the inlet-perforated pipe. There are two short perforated pipes between the first and the third chamber. Both ends of these short perforated pipes are open; therefore, these pipes allow the flow of the exhaust gas from the first chamber to the third chamber, and also into the second chamber through the perforations. Similarly, there are two long perforated pipes between the first and the fourth chambers. The end of the long perforated pipes facing the first chamber are closed, whereas, the ends facing the fourth chamber are open. Therefore, the exhaust gases in the second chamber are sent to the fourth chamber only through the perforation on these pipes. Finally, the exhaust gases in the fourth chamber are discharged into the air through the outlet-perforated pipe. Besides, sound absorbing materials which are made of

glass fibres are placed in the first and fourth chamber between a perforated plate and outer circular walls as shown in Figure 6.2

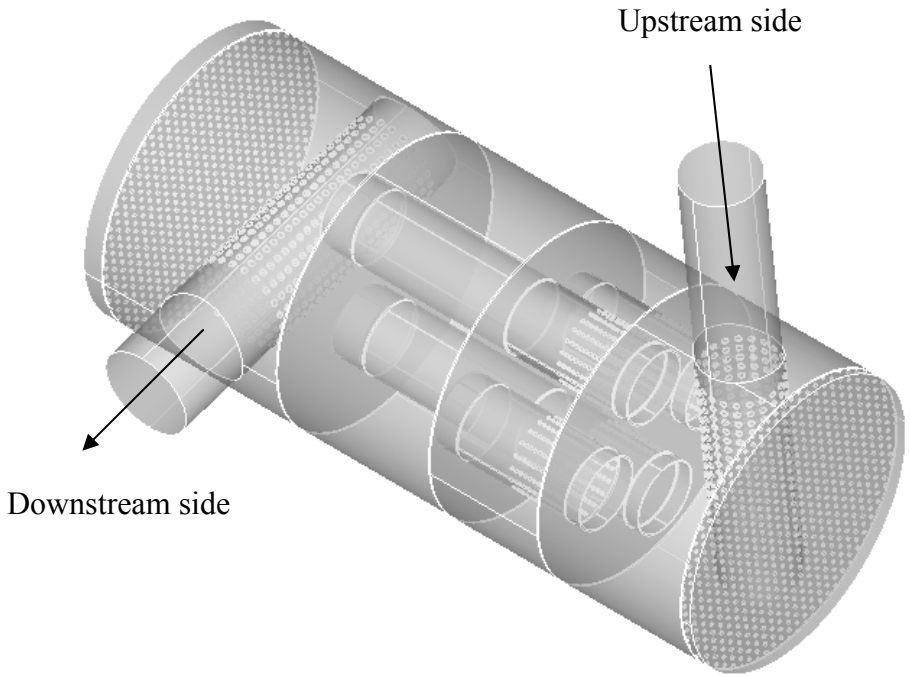

Figure 6.1 – General view of the muffler on HMK 200W-3 wheeled excavator

6.2 Numerical Analysis with Msc.Actran

Three-dimensional finite element analysis is performed on the muffler structure under study. Constructed FE model of the current muffler is composed of 274274 tetrahedral elements and 48949 nodes as shown in Figure 6.3. Acoustic analysis is carried out by following the modelling steps explained in Chapter 3. The perforated ducts are modelled using transfer admittance boundary condition and the transfer impedance of the perforation is estimated by Mechel's formula. Perforations are modelled as uniform perforation with square-grid. Sound absorbing material is modelled as rigid porous material with material density of 100 kg/m^3 and flow resistivity of 5000 rayl/m. The flow is not considered in the analysis since the

experiment is conducted in the absence of mean flow. The fluid medium inside the muffler is air with sound speed c = 348.7 m/s and ρ = 1.01 kg/m^3. FEA is performed for a frequency range of 5-2000 Hz.

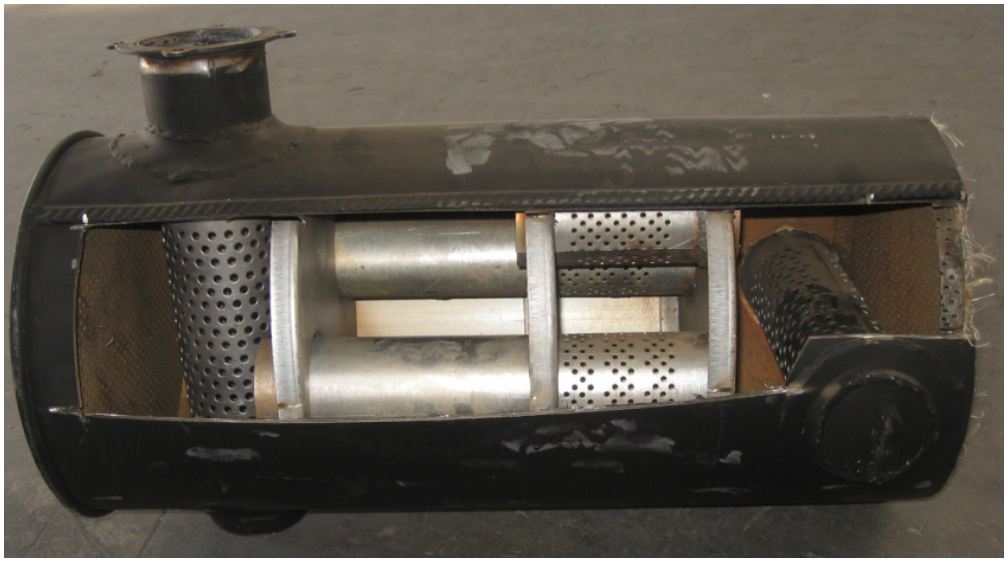

Figure 6.2 – General view of muffler on HMK 200W-3 wheeled excavator

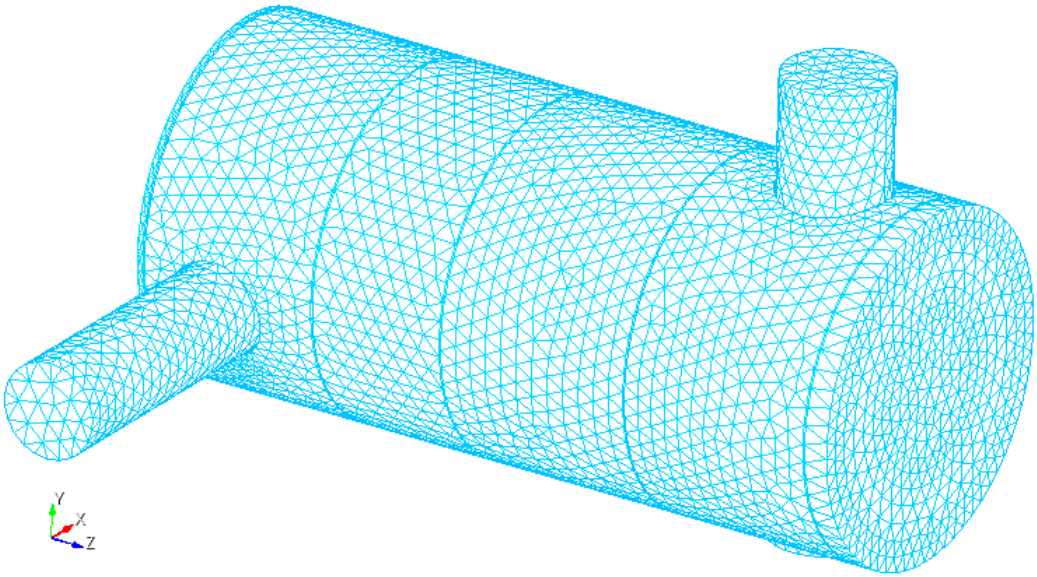

Figure 6.3 – FE model of the muffler on HMK 200W-3 wheeled excavator

6.3 Transmission Loss Experiment with Two-Load Method

The experiments are carried out using two-load method in the designed test setup at test facilities of Hidromek Inc. as shown in Figure 6.4. All the measurements are performed with white noise excitation. Spectral analysis is carried on the Soundbook measurement system with the following parameters: Sample record length 40.96 s, Number of averages: 128, Sampling frequency: 6400 Hz, Window type: Hanning. The room temperature is also measured to calculate speed of sound. The microphone spacing, 50 mm and 60 mm were used for the upstream and downstream impedance tubes, respectively. Therefore, all the results of measurements presented below are valid for frequencies between about 70 Hz and 2250 Hz, that is, only plane waves are propagating in the impedance tubes between these frequencies.

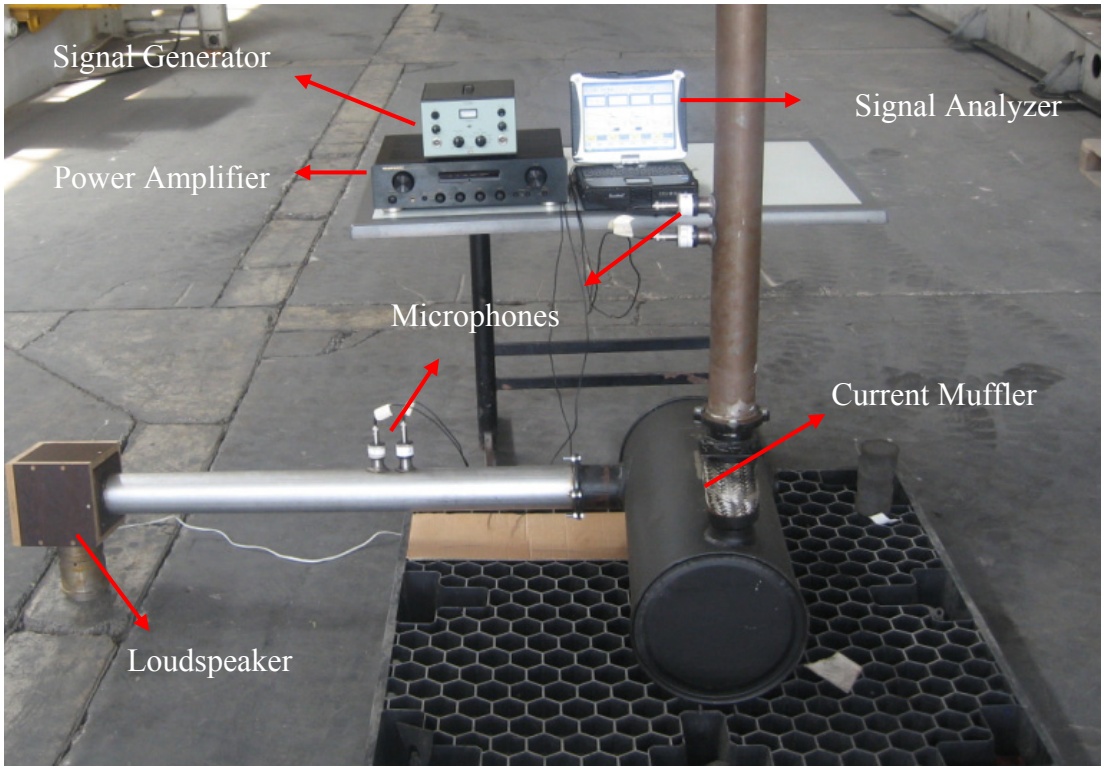

Figure 6.4 – Transmission loss setup used for the muffler of interest

6.4 Comparison between Experimental and Numerical Results

Transmission loss result from the FEA with Msc.Actran is plotted on the Figure 6.5 for comparison with the experimental result using two-load method. The cut-on frequencies calculated by using Equation (3.2) for the higher order modes in the chambers are also plotted as vertical lines in Figure 6.5.

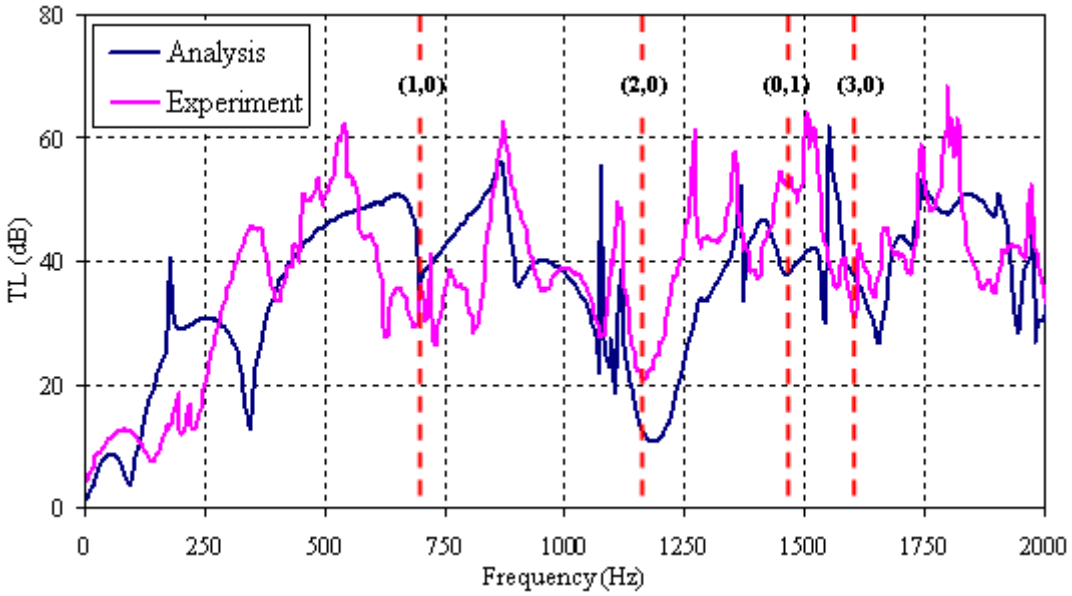

Figure 6.5 – Transmission loss of the muffler of interest

Experimental result is shown to be in reasonable agreement with the numerical prediction in the frequency range of interest. Although analysis result captures the trend, a frequency shift between prediction and measurement is observed in the plane wave region. The main reason for the difference may be attributed to the complexity of the muffler structure in the form of multiple connectivity among the reactive perforated elements. Although higher order modes are propagating at mid- and high frequencies, analysis result is in a good agreement with the experiment with little frequency shift between the curves. The difference between the numerical and

experimental results in high frequencies is thought to be due to the modelling of sound absorbing material. Since there is no experimental data for the characteristic impedance and wave number, approximate values are used for the absorbing material. The other reasons may be due to the non-uniform perforation used in the muffler which can not be modelled by Mechel's formula. Neglected viscous effects and some minor geometrical differences of the production muffler from the model can also lead to some deviations between the transmission loss results.

6.5 Effect of Temperature and Flow on Transmission Loss

It is important to take the effect of the variables dependent on operating condition of muffler on the machine. The most two important variables are exhaust gas temperature and the exhaust gas velocity. Transmission loss of the muffler has been predicted and compared with the experimental results at room temperature without flow. However, the exhaust gas in the muffler is at much more elevated temperatures, nearly 600 ºC and the gas flow velocity is nearly at 0.2 Mach. Therefore, temperature and flow effects on transmission loss are investigated numerically with Msc.Actran and the results are presented in Figures 6.6 and 6.7.

Transmission losses of the muffler at different temperature are calculated in Msc.Actran and shown in Figure 6.6. The primary effect of a change in temperature of the medium is the corresponding change in the speed of sound. The rise of temperature increases the sound speed and therefore the wavelength corresponding to a given frequency. As a result, the transmission loss curve is shifted in the frequency as shown in Figure 6.6.

Figure 6.7 shows the transmission loss curves of the muffler with different flow velocities. It can be observed that there is practically no difference on transmission loss curve for the operation condition of the muffler since the flow values are quite small

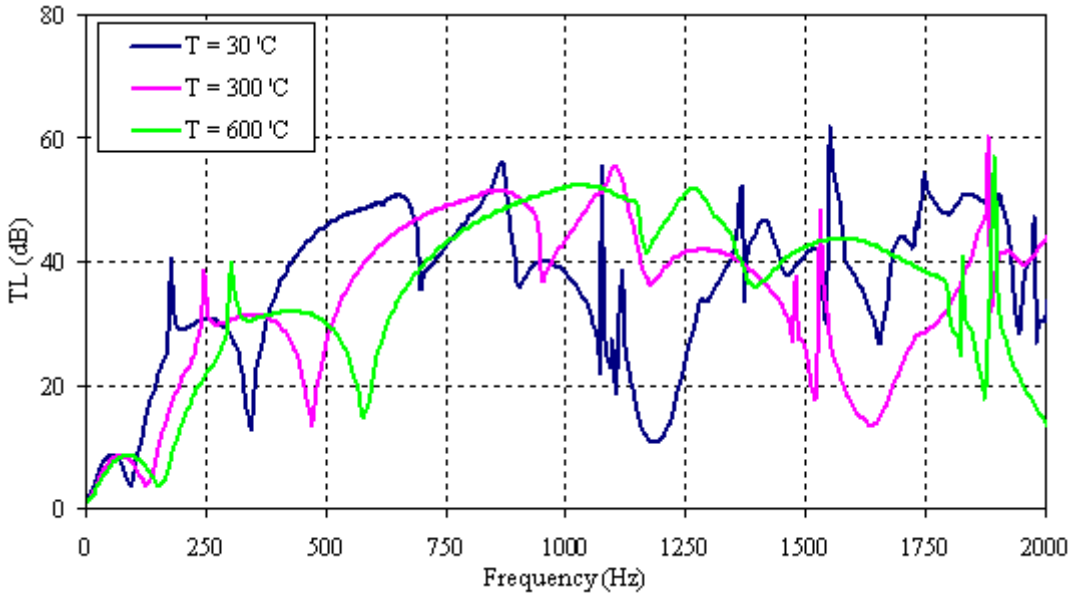

Figure 6.6 – Temperature effect on transmission loss (FEA result)

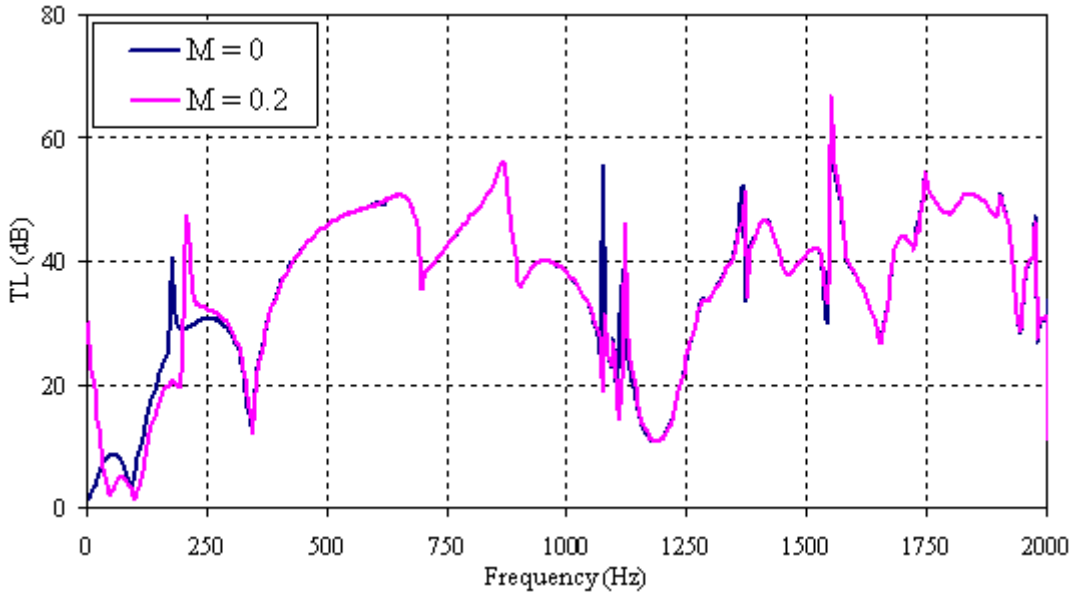

Figure 6.7 – Flow effect on transmission loss (FEA result)

CHAPTER 7

EXPERIMENTAL RESULTS

Experiments are conducted on HMK 200W-3 wheeled excavators, manufactured by Hidromek Inc. Experiments are composed of sound power level determination tests with exterior noise spectral analysis and insertion loss measurement. Sound power level test is performed with muffler and without muffler to evaluate the acoustic performance of the muffler. Furthermore, insertion loss is also measured.

7.1 Airborne Sound Power Level Determination

Exterior sound power level of the excavator is determined according to test procedures described in international standard, ISO 6393[41]. Measurements are carried out in free field where test site has hard reflecting surface i.e. asphalt approximating semi anechoic conditions. Six measurement points, which are shown in Figure 7.1, are drawn on the test surface. These measurement points describe a hypothetical hemisphere, whose radius is determined by machine basic length, which is defined as the machine longitudinal length without movable parts. The corresponding hemisphere radius is 16 m, which is stated in ISO 6393 [41] for basic lengths greater than or equal to 4 m but less than 8 m.

ISO 6393 states that at least three sound levels are to be measured simultaneously at six measurement points. Therefore, a total of three ½ inch G.R.A.S. Type 26CA free field microphones (serial numbers: 86571, 86577, 86679) are used with the Soundbook measurement system (serial number: 7BKCBB81615). The measurement system is calibrated with G.R.A.S. sound level calibrator model 42AB (serial

number: 31513), which supplies a pure tone at 1 kHz with sound pressure level of 114 dB. Microphones are positioned towards the centre of the hypothetical hemisphere. At each position, the background noise is recorded. At least 10 dB difference between measured sound level and the background noise is required to take reliable measurements.

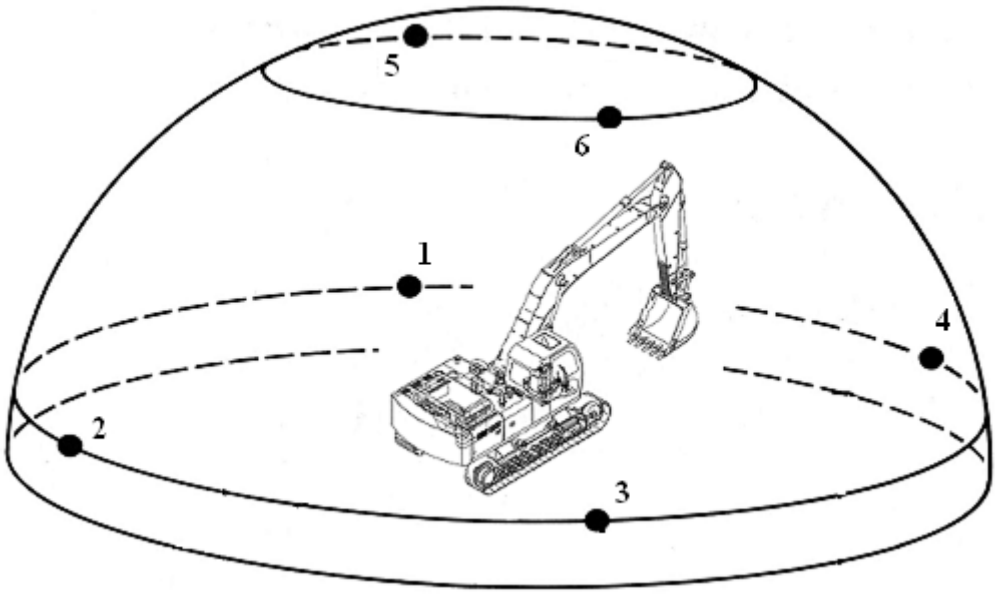

Figure 7.1 – Measurement points for sound power level test

The test machine is located at the centre of the hypothetical hemisphere for static test conditions. The excavator is kept stationary and engine is running at a speed at which maximum net engine power is obtained; therefore, engine revolution speed is set to high idle that is 1800 rpm.

Sound power level determination is carried using the formulae given below:

$$L_{WA} = L_{pA} + 10\log(S) \tag{7.1}$$

where L_{WA} is the A-weighted sound power level of the excavator in decibels, and L_{pA} is the energy average of the time-averaged A-weighted sound pressure levels on the measurement surface in decibels and S is the area of the hemispherical measurement surface.

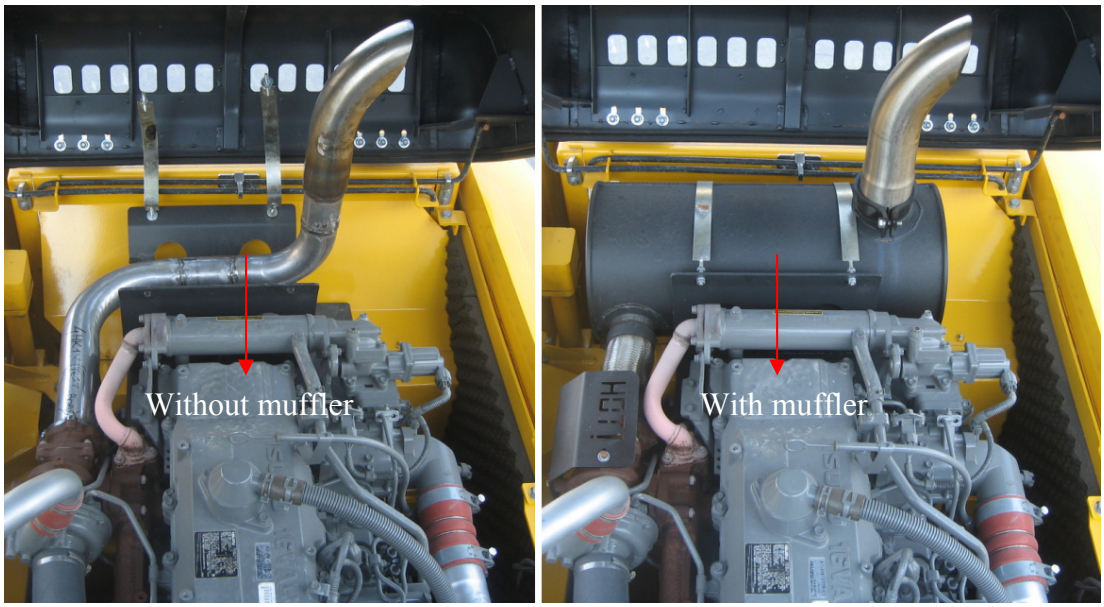

Figure 7.2 – Installation configurations of the muffler for measurements

The sound power level measurements are performed with muffler and without muffler as shown in Figure 7.2. Average sound pressure levels measured on the measurement surface and calculated sound power level of the excavator with muffler and without muffler are tabulated in Table 7.1. The exhaust muffler reduces the sound power level of the excavator by about 9.6 dBA compared to the test results for the configuration conducted without muffler. This reduction could also be named as insertion sound power level difference according to ISO 11820 [42]. This reduction in sound power level means that sound power of the excavator is reduced by 89%. Furthermore, it can be observed that sound pressure level differences vary for each measurement points due to the directivity effect of the exhaust noise.

Table 7.1 – Sound power level of HMK 200W-3 with and without muffler (dBA)

	without muffler		with muffler	
Measurment Points	L_{pA}	L_{WA}	L_{pA}	L_{WA}
1	69.0	108.2	64.6	98.6
2	78.4		66.1	
3	79.6		65.8	
4	72.5		64.8	
5	75.5		68.9	
6	73.9		67.3	

Sound pressure levels are also recorded in constant bandwidth, in a range from 0 to 5 kHz. Hanning window, 128 linear averages with 1601 lines is applied for spectral analysis. By using Equation (7.1), sound power level spectrums are determined and shown in Figure 7.3. It can be easily observed that the muffler is more effective in higher frequencies than lower frequencies. The same graph has been plotted in Figure 7.4 for further investigation of spectral content of the noise emitted by excavator in low frequencies. From the noise control point of view, the frequency at which more sound energy is emitted is essential. Therefore, the peaks which are above 75 dBA for the measurement with muffler configuration are considered here.

It is observed that there are some distinct peaks with little difference in sound power levels between configurations with muffler and without muffler in Figure 7.4. These frequencies are about 200 Hz, 255 Hz, 270 Hz, 285 Hz, 360 Hz, 480 Hz, and 540 Hz. This may be due to acoustical ineffectiveness of the exhaust muffler or external sound sources. Therefore, these frequencies are evaluated with the noise source frequencies in terms of machine operational frequencies.

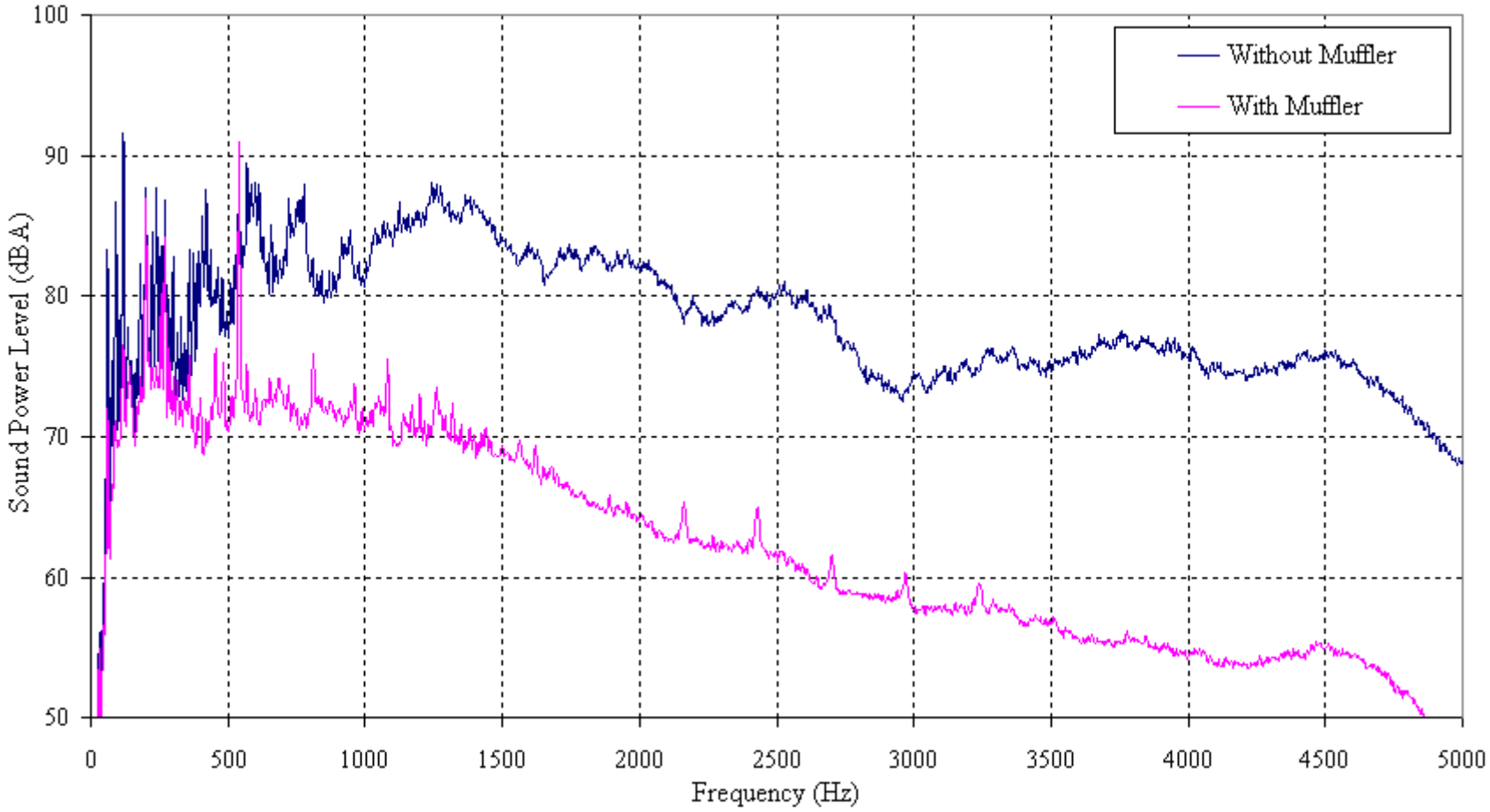

Figure 7.3 – A-weighted sound power level of the excavator with and without muffler up to 5 kHz

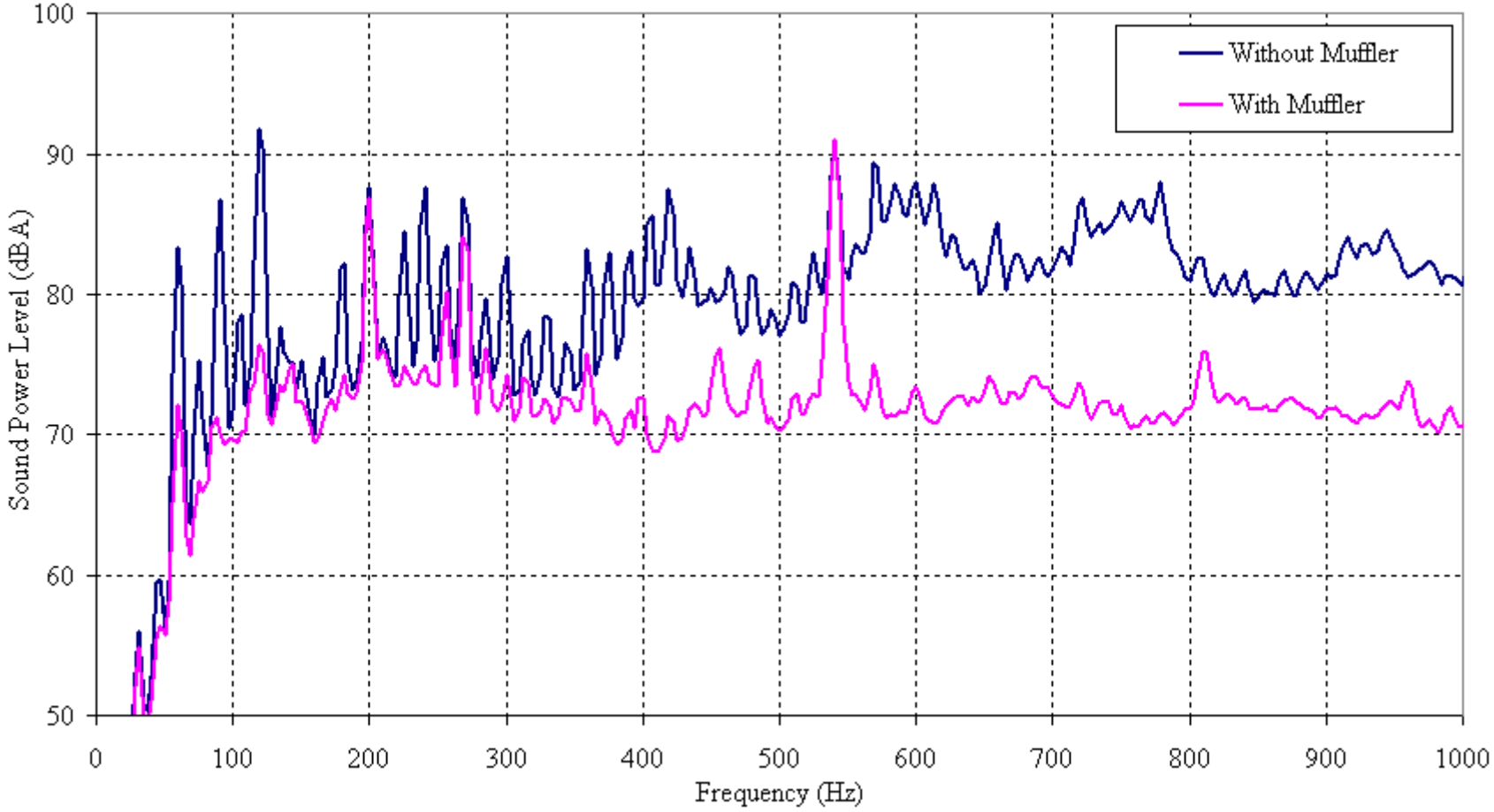

Figure 7.4 – A-weighted sound power level of the excavator with and without up to 1 kHz muffler

Dominant noise sources of HMK 200W-3 wheeled excavator are known as: the cooling fan, the engine, and the hydraulic pump. Noise due to fan is very intense at the blade passage frequency, which is direct function of the number of blades and the fan speed:

$$f_{fan} = \frac{B\Omega}{60} \tag{7.2}$$

where f_{fan} is the blade passage frequency of the fan in Hertz , B is the number of blades and Ω is the rotational speed in revolutions per minute (rpm). The cooling fan of the engine used in the excavator has 7 blades and it is connected to the engine by a belt drive with 0.95-speed ratio. Hence, the fundamental blade passage frequency of the cooling fan is found as 199.5 Hz while engine rational speed is kept at 1800 rpm.

Similarly, noise due to pump occurs at discrete-frequency tones:

$$f_{pump} = \frac{m\Omega}{60} \tag{7.3}$$

where f_{pump} is the operational frequency of the pumps in Hertz, and m is the pumping events per rotation. The excavator has two piston type hydraulic pumps, which are connected in series. They have 9 pistons and are directly connected to the engine. So, the fundamental operational frequency of the pump is found as 270 Hz.

The excavator has four-cycle, four-cylinder, direct injection with turbocharger diesel engine. In four-cycle engines each cylinder fires once every other revolution of the drive shaft. Hence, combustion noise of the engine occurs at cylinder firing frequency, $f_{cylinder}$:

$$f_{cylinder} = \frac{\Omega}{120} \tag{7.4}$$

The exhaust noise spectrum contains strong tones associated with the rate of cylinder firing. However, the engine firing rate is generally the strongest tone in exhaust noise spectrum:

$$f_{engine} = \frac{N\Omega}{120} \tag{7.5}$$

where f_{engine} is engine firing frequency and N is the number of cylinders in the engine. It is evident that 60 Hz is the fundamental engine firing frequency.

The comparison shows that 200 Hz corresponds to the fundamental blade passage frequency of the cooling fan; whereas, 270 Hz and 540 Hz correspond to fundamental hydraulic pump operational frequency and its second harmonics, respectively. Since pump and cooling fan are the predominant noise sources, it is reasonable that there is a little change in sound power level at these frequencies between the measurements with muffler and without muffler. However, the other frequencies, which are 255 Hz, 285 Hz, 360 Hz and 480 Hz, are all related with cylinder firing frequencies or engine firing frequencies. Hence, it has been thought that muffler is not effective is at these frequencies.

7.2 Insertion Loss Measurement

The measurement of insertion loss is made by measuring the sound pressure level difference at the same measurement point without and with muffler according to ISO 11820 [42]. One microphone is placed 1.5 m away from the tailpipe end of the exhaust muffler to minimize the near field effects, and at a 45º angle with pipe axis to avoid the influence of exhaust gas flow. Figure 7.5, which shows insertion loss in

one-third-octave band frequencies, gives general acoustic attenuation performance of the muffler. It can be observed that insertion loss is low below 500 Hz.

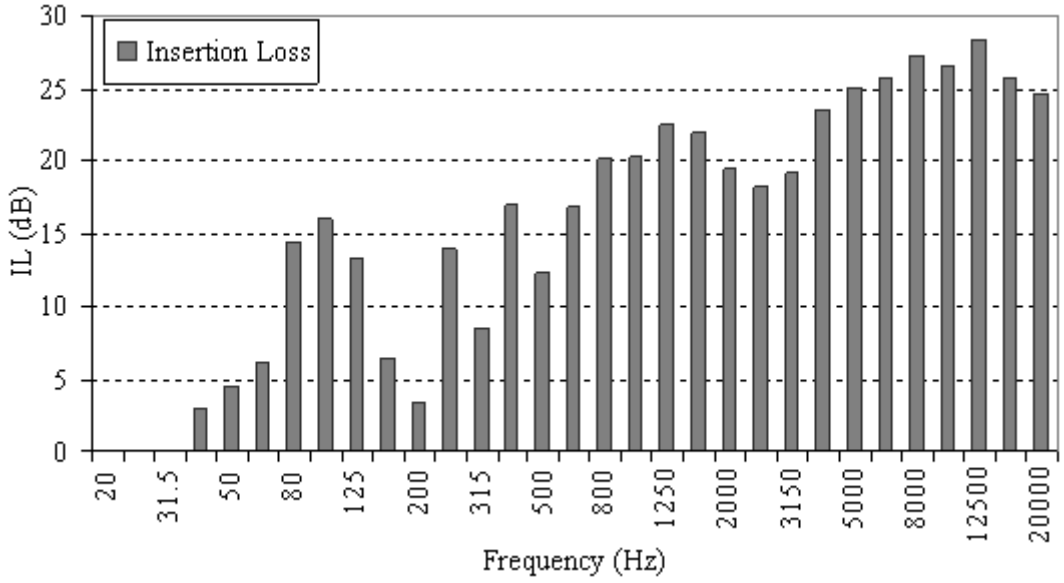

Figure 7.5 – Insertion loss of the muffler of interest in 1/3 octave bands

A preliminary survey for insertion loss can be achieved in octave band analysis. It is, however, not sufficient to observe the spectral content of insertion loss in detail. Therefore, sound pressure levels are also recorded in constant bandwidth in a range from 0 to 2.5 kHz. Hanning window, 128 linear averages with 1601 lines is applied for spectral analysis. Hence, the insertion loss can be shown with about 1.5 Hz frequency resolutions in Figure 7.6. It can be observed that insertion loss has some peaks especially at low frequencies. The same graph has been plotted up to 1 kHz in Figure 7.7 to identify the peak frequencies. It is evident that there are peaks at every 15 Hz intervals in insertion loss curve. This frequency corresponds to the cylinder firing frequency. Evaluation of these spectra reveals that insertion losses are high especially at the fundamental cylinder and engine firing frequencies and their few harmonics. It can also be observed that the insertion loss is low for the frequencies,

namely 255 Hz, 285 Hz, 360 Hz and 480 Hz, at which the muffler is found as ineffective from the sound power measurements.

Temperature of the exhaust gases in the muffler during the insertion loss measurement is found as nearly 300 ºC. The transmission loss of the muffler is calculated for this temperature with taking 0.2 Mach flow into account in Msc.Actran. Figure 7.8 compares measured insertion loss of the muffler with the calculated transmission loss. It can be observed that the quantitative and spectral behaviour of the transmission loss is different from the insertion loss. It is due to the fact that insertion loss gives acoustical performance of the muffler including the interaction of the source and termination impedances. However; transmission loss is a property of the muffler only.

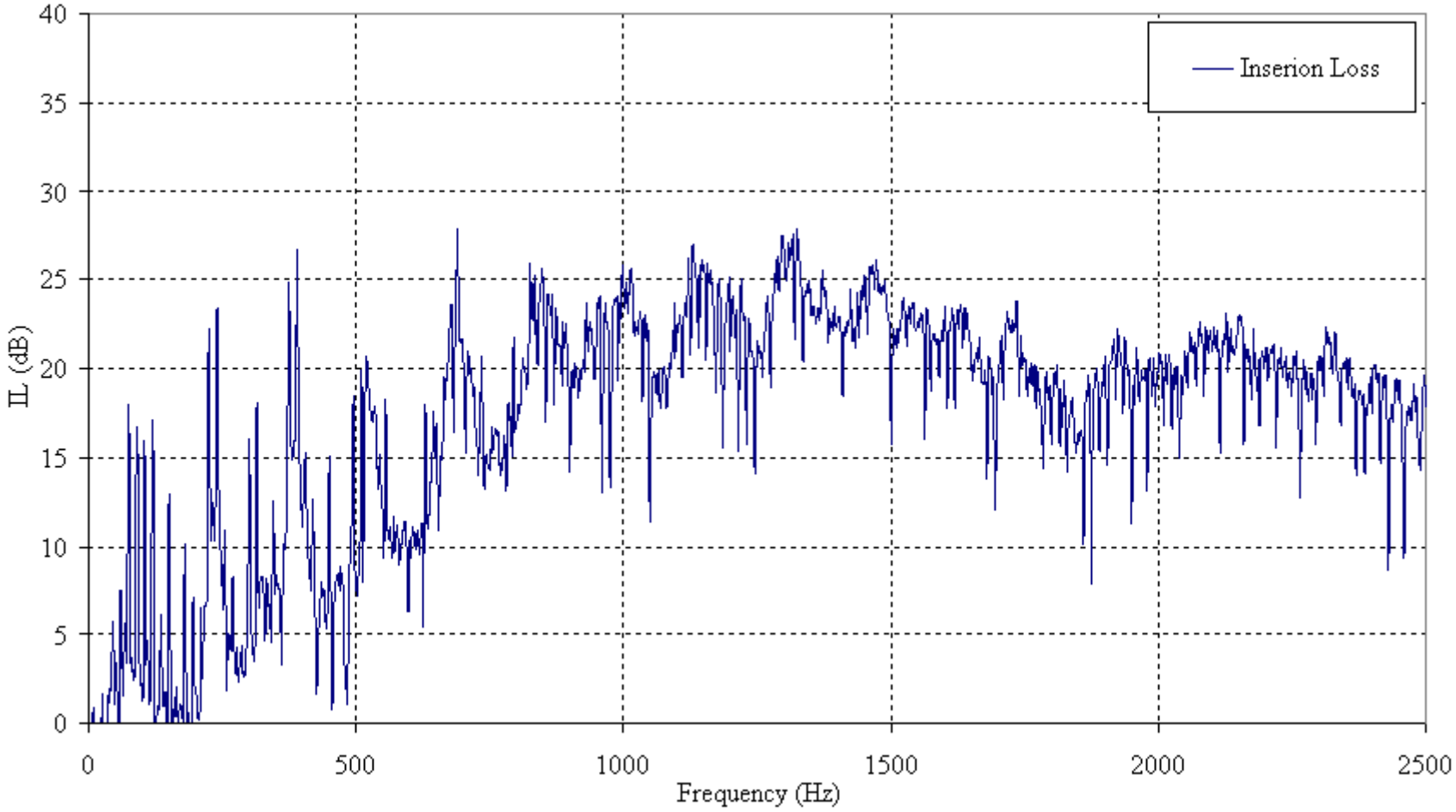

Figure 7.6 – Insertion loss measurement result for the muffler of interest up to 2.5 kHz

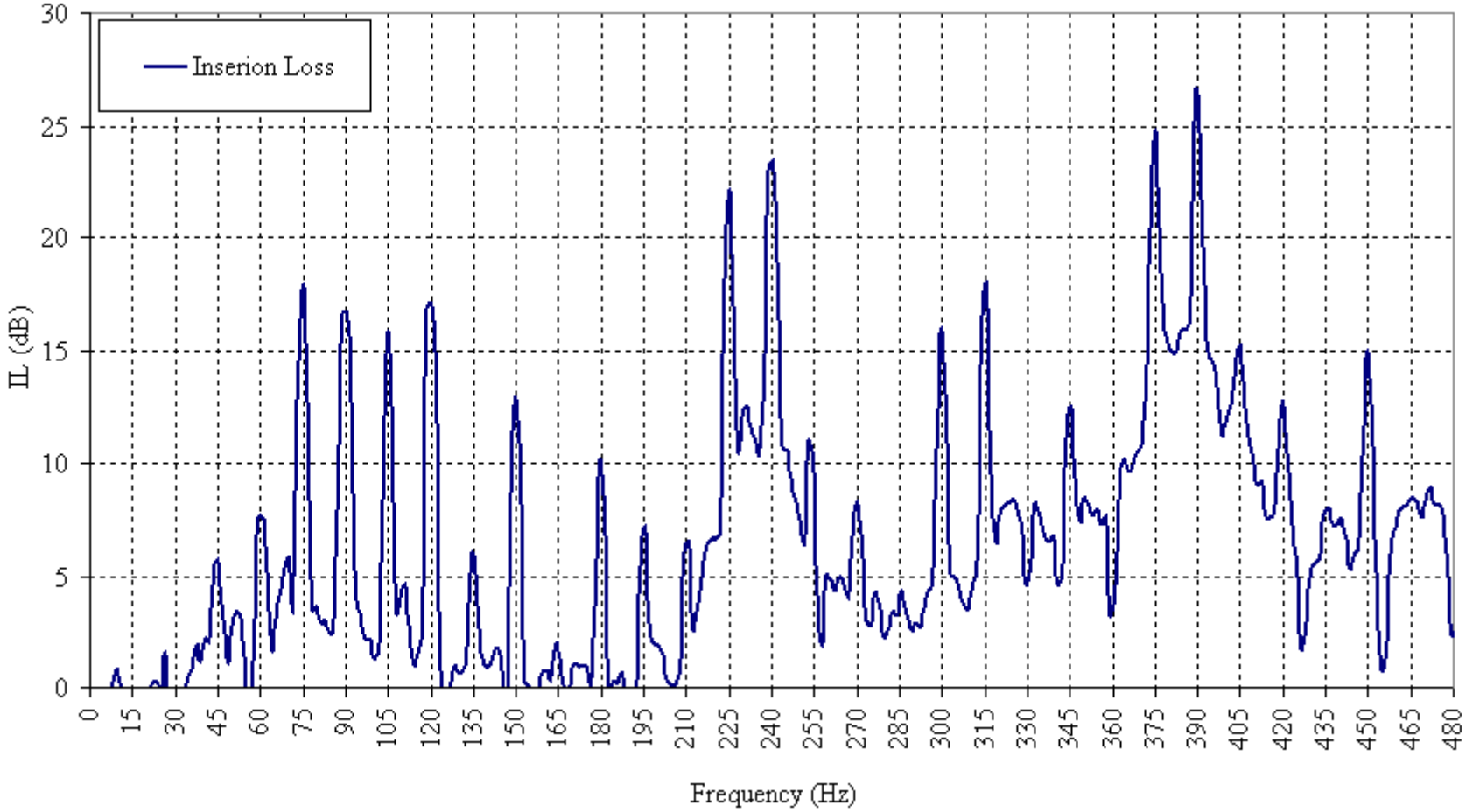

Figure 7.7 – Insertion loss measurement result for the muffler of interest up to1 kHz

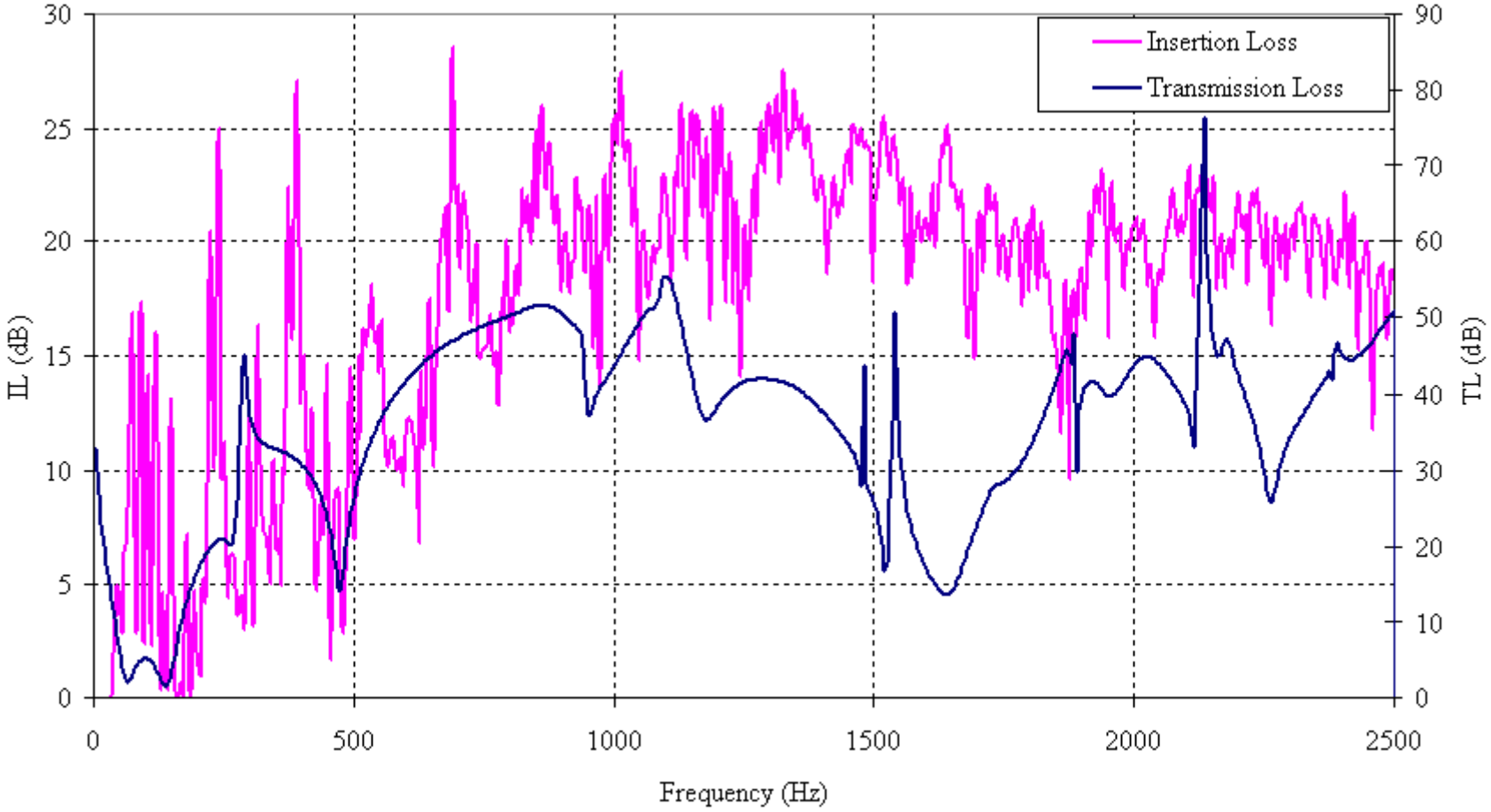

Figure 7.8 – Comparison of measured insertion loss with transmission loss predicted by Msc.Actran

CHAPTER 8

DISCUSSIONS AND CONCLUSIONS

Main area of interest in this research study is acoustical evaluation of exhaust muffler for earth-moving machinery leading to new design tips. Acoustical characteristics of the exhaust muffler of interest are investigated both computationally and experimentally. Hence, discussions and conclusions are presented in this chapter, entitled, namely, finite element modelling, experimental methods and future work.

8.1 Finite Element Modelling

FEM is used for the prediction of transmission losses due to its capability of analyzing complex muffler configurations. Modelling of perforation and sound absorbing material is essential in acoustical analysis of exhaust mufflers; therefore, modelling approaches are presented first.

Perforations are modelled by admittance boundary condition, in which transfer impedances are calculated by Mechel's formula. This modelling approach is verified by comparing the transmission loss result for three-pass perforated muffler with the result of the study performed by Ji and Selamet [36]. This comparison shows that uniform perforation with square grid can be modelled by admittance boundary condition with Mechel's formula effectively. However, modelling of non-uniform perforation should be further investigated.

Two acoustical modelling approaches are considered for sound absorbing material in this study. In the first approach, sound absorbing material is modelled as rigid porous

material which is one of the material models available in Msc.Actran library. The other modelling approach uses complex speed of sound and wave number for modelling. Furthermore, acoustic impedance of perforation in contact with absorbing material is different than of the perforation in contact with air only, which is calculated by Mechel's formula. However, experimental results are needed for the determination of both acoustic impedance contacting with sound absorbing material and complex speed of sound and wave number. Therefore, the first modelling approach with acoustic impedance of perforation in contact with air only is considered throughout the study. This modelling approach is verified by comparing the transmission loss prediction for single-pass perforated muffler with the experimental result obtained in the study by Selamet et al. [37].

The muffler used on HMK 200W-3 wheeled excavator, manufactured by Hidromek Inc. is acoustically analyzed by using the above mentioned modelling approaches for perforation and sound absorbing material. The effect of temperature and flow on transmission loss of the muffler is also investigated by numerical means. It is shown that the transmission loss curve is shifted in the frequency axis due to the change of temperature; whereas, there is nearly no change on transmission loss due to the flow in the medium. Hence, temperature effect should be considered in acoustical design of exhaust muffler.

8.2 Experimental Methods

The present study has developed an experimental setup to measure the transmission loss of the muffler. The experimental setup consists of mainly an impedance tube, a speaker, a signal generator, a power amplifier, four microphones and a signal analyzer. Three experimental techniques are presented for transmission loss measurements, namely, Chung-Blaser method, two-source method and two-load method. These methods are applied to measure transmission loss of the single expansion chamber with extended inlet/outlet. The experimental results are

compared with one-dimensional analytical solution obtained by transfer matrix method. The results are found to be fairly accurate for two-load method in the designed experimental setup. Therefore, two-load method is used for the determination of the transmission loss throughout the study. Experimental result for the muffler of interest is shown to be in reasonable agreement with the transmission loss prediction. This encourages further work with other exhaust mufflers used on the other types of earth-moving machinery.

Sound power level of the excavator was also determined with muffler and without muffler. A 9.6 dBA noise reduction is observed in the airborne sound power level of the excavator after installation of the muffler. Furthermore, spectral analysis of the noise emitted by the excavator is carried out. After comparative evaluation of the high-energy peak frequencies with known noise source frequencies, the frequencies at which the current muffler is ineffective are identified.

Insertion loss of the muffler of interest is also measured and compared with transmission loss prediction by finite element method. It is seen that the insertion loss curve is drastically different from transmission loss curve as expected. A gross error is made if it is assumed that insertion loss and transmission loss are equal.

8.3 Future Work

The effect of muffler parameters; such as perforation length, porosity, length of the expansion chamber and the end cavities, duct extensions into the end cavities, on acoustic attenuation performance of the muffler of interest should be investigated by experimental and numerical means. The results can be used to improve the acoustical performance of the current muffler. Furthermore, parametric finite element analysis could then be used to reach an optimum design in terms of transmission loss.

Complex characteristic impedance and complex wave number for the sound absorbing material used in the muffler needs to be determined experimentally for accurate acoustical modelling. Furthermore, the acoustic impedance of the perforation in contact with fibrous material needs to be measured and these inferred from the experiments are then used for the predictions of transmission loss of the muffler.

Acoustic analysis and transmission loss measurement can be extended from the muffler to diesel particulate filter and diesel oxidation catalyst, which will be in use in near future for exhaust emission reduction. The present study can then be served as a design guide for the new mufflers.

In addition to the acoustic performance, the flow efficiency in the exhaust system is important to maintain relatively low backpressure. Muffler would then be aerodynamically analyzed with the help of proper finite element software and the predicted backpressure needs to be verified by experiments. If the backpressure were not sufficiently low, a new muffler design should be considered.

REFERENCES

[1] SAE J1116 REV. NOV 2004: Categories of Off-Road Self-Propelled Work Machines

[2] E.A. Avallone, T. Baumaister III, Marks' Standard Handbook for Mechanical Engineers, 10th edition, McGRAW-HILL International editions, 1997.

[3] ISO 6165:2006 : Earth-moving machinery - Basic types - Identifications and Terms and Definitions

[4] Directive 2000/14/EC of the European Parliament and of the Council, on the Approximation of the Laws of the Member States Relating to the Noise Emission in the Environment by Equipment for Use Outdoors, 2000

[5] D. D. Davis, G. M. Stokes, D. Moore and G. L. Stevens, N.A.C.A. Report 1192, "Theoretical and Experimental Investigation of Mufflers with Comments on Engine-exhaust Muffler Design", 1954

[6] J. Igarashi and M. Toyoma, "Fundamentals of Acoustical Silencers (I)", Report No. 339, Aeronautical Research Institute , University of Tokyo, 223-241, 1958

[7] T. Miwa and J. Igarashi "Fundamentals of Acoustical Silencers (II)", Report No. 344, Aeronautical Research Institute , University of Tokyo, 67-85, 1959

[8] A. V. Sreenath and M. L. Munjal, "Evaluation of Noise Attenuation due to Exhaust Mufflers", Journal of Sound and Vibration 12, 1-19, 1970

[9] M. L. Munjal, “Analysis and Design of Mufflers – An Overview of Research at the Indian Institute of Science” Journal of Sound and Vibration 211, 425-433, 1998

[10] M. L. Munjal, “Velocity ratio cum transfer matrix method for evaluation of a muffler”, Journal of Sound and Vibration 39, 105-119, 1975

[11] M. L. Munjal, “Acoustics of Ducts and Mufflers With Application to Exhaust and Ventilation System Design”, 1st edition, John Wiley & Sons, 1987

[12] F. P. Mechel (Ed.), “Formulas of Acoustics” 2nd edition, Springer-Verlang, 2008

[13] J. W. Sullivan and M. J. Crocker, “Analysis of Concentric Tube Resonators Having Unpartitioned Cavities”, Journal of the Acoustical Society of America 64, 207-215, 1978

[14] J. W. Sullivan, “A Method for Modelling Perforated Tube Muffler Components I. Theory”, Journal of the Acoustical Society of America 66, 772-778, 1979

[15] T. Elnady, “Modelling and Characterization of Perforates in Lined Ducts and Mufflers”, Doctoral Thesis submitted to The Royal Institute of Technology, Sweden, 2004

[16] A. Selamet and P. M. Radavich, “The Effect of Length on the Acoustic Attenuation Performance of Concentric Expansion Chambers”, Journal of Sound and Vibration 201, 407-426, 1997

[17] A. Selamet and Z. L. Ji, “Acoustic Attenuation Performance of Circular Expansion Chambers with Offset Inlet/Outlet: I. Analytical Approach”, Journal of Sound and Vibration 213, 601-617, 1998

[18] A. Selamet and Z. L. Ji, “Acoustic Attenuation Performance of Circular Flow-Reversing Chambers”, Journal of the Acoustical Society of America 104, 2867-2877, 1998.

[19] C. J. Young and M. J. Crocker, “Prediction of Transmission Loss in Mufflers by the Finite-Element Method”, Journal of the Acoustical Society of America 57, 144-148, 1975

[20] C. J. Young and M. J. Crocker, “Acoustical Analysis, Testing, and Design of Flow-Reversing Muffler Chamber”, Journal of the Acoustical Society of America 60, 1111-1118, 1976

[21] S. Bilawchuck and K. R. Fyfe, “Comparison and Implementation of Various Numerical Methods used for Calculating Transmission Loss in Silencer Systems”, Applied Acoustics 64, 903-916, 2003

[22] T. W. Wu, P. Zhang, C. Y. R. Cheng, “Boundary Element Analysis of Mufflers with an Improved Method for Deriving the Four-pole Parameters”, Journal of Sound and Vibration 217, 767-779, 1998

[23] T. W. Wu, P. Zhang, C. Y. R. Cheng, “A Direct Mixed-body Boundary Element Method for Packed Silencers”, Journal of the Acoustical Society of America 111, 2566-2572, 2002

[24] O. Z. Mehdizadeh and M. Paraschivoiu, “A Three-dimensional Finite Element Approach for Predicting the Transmission Loss in Mufflers and Silencers with no Mean Flow, Applied Acoustics 66, 902-918, 2005

[25] A. F. Seybert and D. F. Ross, “Experimental Determination of Acoustic Properties using a Two-microphone Random-excitation Technique” Journal of the Acoustical Society of America 61, 1362-1370, 1977

[26] J. Y. Chung and D. A. Blaser, “Transfer Function Method of Measuring in-duct Acoustic Properties. I. Theory “ Journal of the Acoustical Society of America 68, 907–913, 1980

[27] T. Y. Lung and A. G. Doige, “A Time Averaging Transient Testing Method for Acoustic Properties of Piping Systems and Mufflers with Flow” Journal of the Acoustical Society of America 73, 867-876, 1983

[28] M. L. Munjal and A.G. Doige, “Theory of Two Source Location Method For Direct Experimental Evaluation of the Four-Pole Parameters of An Aeroacoustic Element” Journal of Sound and Vibration 141, 323-333,1990

[29] M. J. Crocker (Ed.), “Handbook of Noise and Vibration Control”, 1st edition, John Wiley & Sons, 2007

[30] L. J. Eriksson, “Higher order mode effects in circular ducts and expansion chambers”, Journal of the Acoustical Society of America 68, 1980

[31] R. Glav and M. Åbom, “A General Formalism for Analyzing Acoustic 2-Port Networks”, Journal of Sound and Vibration 202, 739-747, 1997

[32] Actran User’s Manual, Free Field Technologies, 2005

[33] I. Lee, A. Selamet, N. T. Huff, “Acoustic Impedance of Perforations in contact with Fibrous Material”, Journal of the Acoustical Society of America 119, 2785-2797, 2006

[34] “How to Use Mechel’s Formula within Actran”, Free Field Technologies, 2007

[35] Z. L. Ji and A. Selamet, “Boundary Element Analysis of Three-pass Perforated muffler”, Noise Control Engineering Journal 48, 151-156, 2000

[36] M. E. Delany and E. N. Bazley, “Acoustical Properties of fibrous absorbent materials”, Applied Acoustics 3, 105-116, 1970

[37] A. Selamet, I. J. Lee, Z. L. Ji, N. T. Huff, “Acoustic Attenuation Performance of Perforated Absorbing: Silencers”, Society of Automotive Engineers, 2001-01-1435

[38] Y. Ryu and M. Choi, “Transmission Loss Measurement of the Exhaust System Using 4-Micropones with Impedance Tube”, 18th International Congress on Acoustics, 2004

[39] ISO 10534-2: Determination of sound absorption coefficient and impedance in impedance tubes - Transfer Function Method

[40] ASTM E 1050: Standard Test Method For Impedance And Absorption of Acoustical Materials Using A Tube, Two Microphones and A Digital Frequency Analysis System

[41] ISO 6393: Acoustics – Measurement of Exterior noise emitted by earth-moving machinery – Static Test Conditions, 2008

[42] ISO 11820: Acoustics – Measurements on silencers in situ, First Edition, 1996